Crustal wedging triggering recent deformation in the Andean thrust front between 31°S and 33°S: Sierras Pampeanas-Precordillera interaction

J. Vergés,[1] V. A. Ramos,[2] A. Meigs,[3] E. Cristallini,[2] F. H. Bettini,[4] and J. M. Cortés[2]

Received 13 January 2006; revised 16 October 2006; accepted 15 November 2006; published 1 March 2007.

[1] We document a new model of crustal structure of the Andean front in Argentina where numerous historic earthquakes destroyed the cities of Mendoza in 1861 (M_s = ~7) and San Juan in 1944 (M_w = 7.0). The Cerro Salinas anticline is formed above the west directed Cerro Salinas thrust. An east facing monocline with an amplitude of about 2 km folds the Cerro Salinas thrust and overlying Neogene succession. This monocline is formed above a blind crustal thrust in the basement. Its dip of 14° west is inferred from fold geometry. This thick-skinned east directed blind thrust and the thin-skinned west directed Cerro Salinas thrust define a tectonic wedge; the wedge tip occurs at a depth of 5.4 km. Growth of the monocline after ~8.5 Ma is revealed on multichannel seismic (MSC) profile 31017 (Repsol-YPF). Rates of Cerro Salinas thrust displacement are of the order of 1 mm/yr, whereas vertical uplift of ~0.45 mm/yr results from the combined displacement on the Cerro Salinas thrust and growth of east facing monocline. The lateral extent of the east directed crustal blind ramp corresponds with the along-strike extent of the Eastern Precordillera. When combined with the low displacement rate, a long earthquake recurrence interval is implied. Smaller magnitude earthquakes, however, indicate that segments of the blind thrust ramps ruptured in historic events. If all the segments of the blind thrust ruptured together the fault area is ~7000 km^2 and could produce a M_w ~ 7.7 earthquake. The crustal wedge model provides new constraints on the origin and potential size of earthquakes that threaten the densely populated region.

Citation: Vergés, J., V. A. Ramos, A. Meigs, E. Cristallini, F. H. Bettini, and J. M. Cortés (2007), Crustal wedging triggering recent deformation in the Andean thrust front between 31°S and 33°S: Sierras Pampeanas-Precordillera interaction, *J. Geophys. Res.*, *112*, B03S15, doi:10.1029/2006JB004287.

1. Introduction

[2] Active deformation along the front of the Andes in Argentina between 30°30′S and 32°30′S is characterized by the interaction between thin-skinned and thick thrust fault domains [*Jordan and Allmendinger*, 1986]. Major structural provinces are the west directed Sierras Pampeanas to the east, the west directed Eastern Precordillera in the center, and the east directed Central Precordillera thin-skinned thrust belt to the west (Figure 1). Structures inherited from Paleozoic and older times are preserved in the crust beneath this frontal part of the Andes [e.g., *Cominguez and Ramos*, 1991; *Astini et al.*, 1995].

[3] Basement-involved structures of the Sierras Pampeanas formed above the southern part of the flat subduction segment Nazca plate [*Isacks et al.*, 1982; *Jordan et al.*, 1983; *Smalley and Isacks*, 1987] (inset in Figure 1). Onset of flat slab subduction is indicated by deformation in the Sierras Pampeanas and cessation of volcanic activity between latitudes 27°S and 33°S after ~7 Ma [e.g., *Kay and Abbruzzi*, 1996]. Both the thin-skinned Precordillera and thick-skinned Sierras Pampeanas structures between the city of San Juan in the north and the city of Mendoza in the south show evidence of active deformation, including widespread deformation of Quaternary deposits and recent devastating earthquakes [*Costa and Vita-Finzi*, 1996; *Costa et al.*, 1999, 2000] (Figure 1). The city of Mendoza (presently with 1,025,000 inhabitants) was destroyed in 1861 by a M_s = ~7 earthquake [*Instituto Nacional de Prevención Sísmica (INPRES)*, 1995] and the city of San Juan (presently with 350,000 inhabitants) was also ruined in 1944 by an earthquake of M_w = 7.0 [*Castellanos*, 1944; *Groeber*, 1944; *Alvarado and Beck*, 2006]. The seismic hazard in this segment of the front of the Andes is still significant as demonstrated by recent important earthquakes with M_s over 7.0 damaging the city of Caucete in 1977

[1]Group of Dynamics of the Lithosphere, Institute of Earth Sciences "Jaume Almera", Consejo Superior de Investigaciones Científicas, Barcelona, Spain.
[2]Laboratorio de Tectónica Andina, Departamento de Ciencias Geológicas, Universidad de Buenos Aires, Buenos Aires, Argentina.
[3]Department of Geosciences, Oregon State University, Corvallis, Oregon, USA.
[4]Repsol-YPF, Buenos Aires, Argentina.

0148-0227/07/2006JB004287$09.00

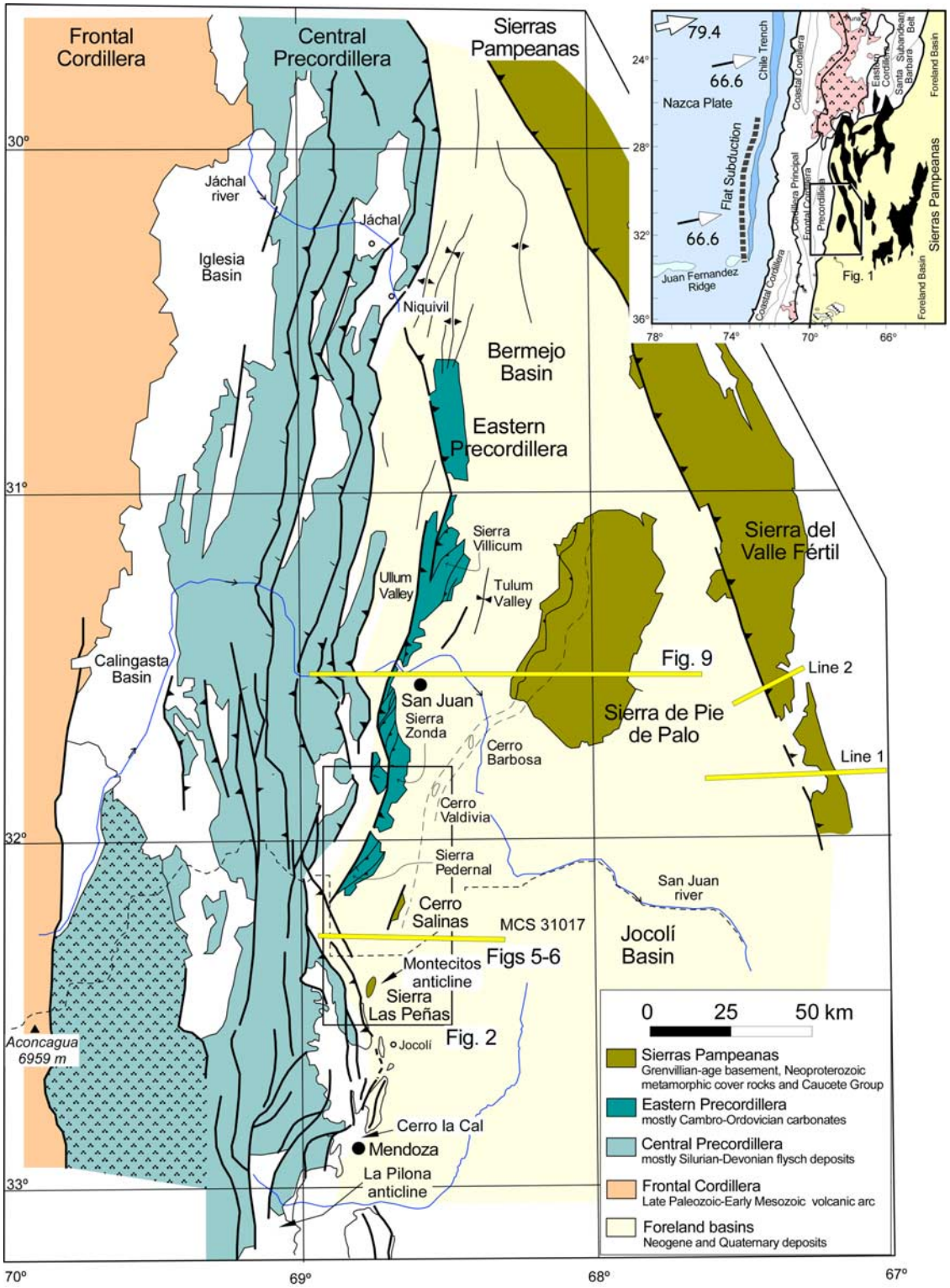

Figure 1. Tectonic map of the front of the Andes between latitudes 30°S and 33°S showing the interactions between west directed Sierras Pampeanas and Eastern Precordillera and east directed Central Precordillera tectonic domains. Location of cross sections, seismic lines, regional profiles, and the map of Figure 2 are shown. The inset map shows the Sierras Pampeanas in black formed between 27°S and 33°S above a flat subduction segment. Black and white arrows are the relative convergence rates (in mm/yr) following NUVEL-1 [*DeMets et al.*, 1990] and GPS data [*Kendrick et al.*, 1999].

(M_s = 7.4) and 1978 [e.g., *INPRES*, 1982; *Kadinsky-Cade et al.*, 1985].

[4] Although the Precordillera and Sierras Pampeanas boundary has been the focus of several studies, the crustal-scale structure is still controversial due to the lack of available subsurface information. The Cerro Salinas, interpreted as the southernmost outcrop of the Western Sierras Pampeanas, displays excellent surface outcrops for both Neogene and Quaternary deposits as well as old, but relatively good, seismic coverage provided by Repsol-YPF company. The study of this region is thus of great interest to unravel the structure of this complex region.

[5] We integrate in this work surface and subsurface geology together with geomorphology around the Cerro Salinas anticline. The interpretation of seismic lines, the analysis of growth strata patterns within the upper part of the Neogene infill of the proximal Jocolí foreland basin, and interpretation of deformed geomorphic surfaces are combined (1) to characterize the shallow and deep structure of the southernmost end of the Eastern Precordillera (latitude 32°S); (2) to constrain the timing of tectonic shortening; (3) to characterize interaction between the Sierras Pampeanas and the Precordillera; and (4) to develop a regional model for crustal deformation and seismogenic sources along a 200-km-long segment of the front of the Andes between the cities of San Juan and Mendoza. Our new model for crustal structure fits well with a large number of geological and geomorphic observables and provides a new perspective on the origin and potential size of earthquakes that threaten this densely populated region of western Argentina.

2. Western Sierras Pampeanas and Precordillera Structure

[6] The Cenozoic structure of the front of the Andes between the cities of San Juan and Mendoza (30°30′S and 32°30′S) comprises two opposed thrust systems [e.g., *Ramos*, 1988]. The Western Sierras Pampeanas and the Eastern Precordillera are underlain by west directed thrust systems whereas the Central Precordillera shows east directed thrusting (Figure 1) [*Figueroa and Ferraris*, 1989; *von Gosen*, 1992; *Ramos et al.*, 1997]. The Eastern Precordillera dies to the north of 30°30′S and beneath the east directed Central Precordillera at 32°30′S to the south at Sierra de las Peñas front [*Costa et al.*, 2000] (Figure 1). The Sierras Pampeanas between 30°S and 32°S are defined by the Sierra de Valle Fértil to the east, the Sierra de Pie de Palo, and by a succession of relatively small hills aligned NNE-SSW, including the Cerro Barbosa and Cerro Valdivia (Figure 1).

[7] Late Cenozoic deformation across Sierras Pampeanas, Eastern Precordillera and Central Precordillera is well known. This Cenozoic deformation overprints a record a prolonged Paleozoic collisional characterized by the complex accretion of different terranes preserved below an unconformity at the base of the Neogene foreland basin deposits [e.g., *Furque and Cuerda*, 1979; *Ramos*, 1988]. Reactivation of these older structures and their control of the Tertiary deformation is now being studied in more detail [e.g., *Alonso et al.*, 2005; *Piñán-Llamas and Simpson*, 2006]. From Cambrian to Late Ordovician times the oceanic lithosphere at the eastern margin of the Precordillera terrane subducted to the east beneath Gondwana deforming its margin by west directed tectonic imbricates involving both basement and cover rocks that formed a foredeep basin thickening to the east [e.g., *Astini et al.*, 1995]. A flip in the subduction direction from east to west took place at Late Ordovician times with the subduction of the western boundary of the Precordillera terrane, which produced an east directed thrust system mostly involving Silurian and Devonian deep marine flysch deposits filling a foredeep basin that thickened to the west [*González Bonorino*, 1973].

[8] The west directed thrust imbricate system is well recognized in the Sierra de Pie de Palo where different tectonic slices carrying Grenvillian age basement and low-grade Neoproterozoic metamorphic cover rocks show a top to the west motion on top of each other [*Galindo et al.*, 2004]. These imbricates overthrust Cambrian carbonates of the Caucete Group above the basal Pirquitas thrust exposed along the western flank of the Sierra de Pie de Palo. This thrust may represent the western boundary of the Sierras Pampeanas during Early Paleozoic times [*Galindo et al.*, 2004]. Deformation in the Paleozoic collisional system migrated to the west [e.g., *Vujovich and Ramos*, 1994; *Pankhurst et al.*, 1998; *Ramos et al.*, 1998; *Ramos and Vujovich*, 2000]. Structures related with these imbricate thrust systems are unconformably overlain by Carboniferous continental deposits [*Ramos et al.*, 1986; *Ramos and Vujovich*, 2000]. Crustal structure established in the Paleozoic therefore exerts a strong control on the present interaction between the thin-skinned Andean thrust front on the west and structures in the east in the Eastern Precordillera and Sierras Pampeanas that involve Early Paleozoic and older rocks.

3. Cerro Salinas Anticline

[9] Eastern Precordilleran structures occur in a narrow belt ~200 km long extending from San Juan on the north to the north of Mendoza on the south (Figures 1 and 2). Cerro Salinas, the southernmost thrust sheet of the Eastern Precordillera, is a relatively small hill mostly formed by the resistant outcrops of Late Proterozoic-Cambrian rocks. These comprise thin marbles and schists of the Caucete Group, with total structural thickness of ~500 m, which were tectonically repeated by west directed imbricate thrusts during the Paleozoic [*Cominguez and Ramos*, 1991] (Figure 3b). The basal thrust of these imbricates is difficult to observe in the field but appears to cut gently folded Neogene strata along the western front of the Cerro Salinas [*Cominguez and Ramos*, 1991]. A highly asymmetric west verging anticline characterizes Neogene strata along strike to the south of the Cerro Salinas (Figure 2). The 45°, west dipping forelimb is narrow whereas the backlimb is more than 6 km wide and dips between 23° and 30° to the east (Figure 3c). Thickness of the exposed Neogene section in the backlimb of the anticline is ~1850 m. This Neogene sequence onlaps the Paleozoic imbricates on the east side of Cerro Salinas, which indicates that a paleotopographic high existed prior to Neogene deposition. To the east and south of the Cerro Salinas, folded and thrusted Quaternary terraces are preserved and help to unravel the character of recent deformation. Clearly the Paleozoic faults were reactivated in

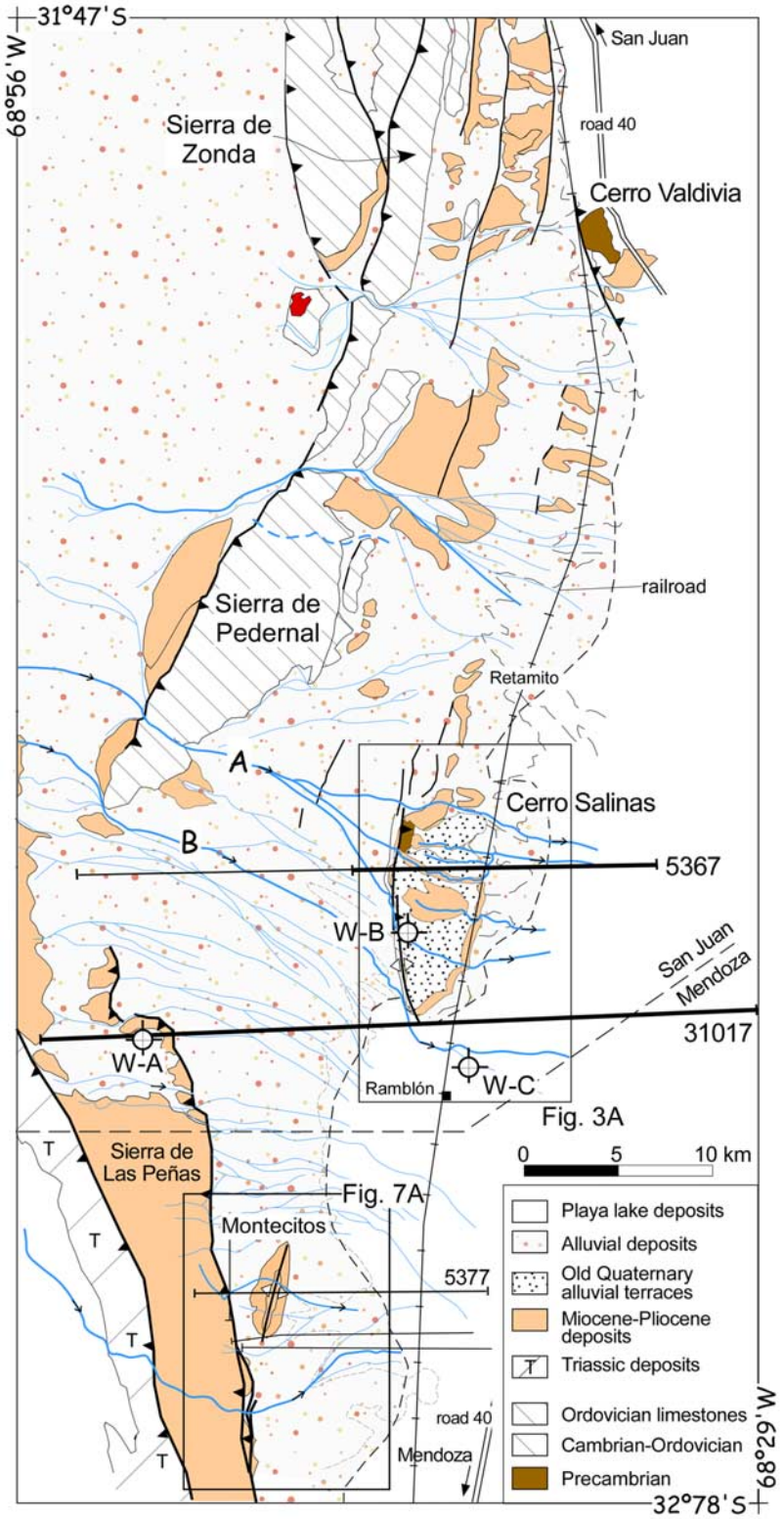

Figure 2. Tectonic and geomorphic map of the west Sierras Pampeanas-Precordillera interaction at Cerro Salinas with location of seismic profiles and exploratory oil wells (labeled as W-A, W-B, and W-C). See the locations of satellite images in Figures 3a and 7a. MCS profile 31017 continues 9 km to the east across the undeformed Jocolí foreland basin. An interpretation of MCS profile 5377 across the Montecitos anticline is shown in Figure 9. The rivers flow from west to east over large alluvial fans.

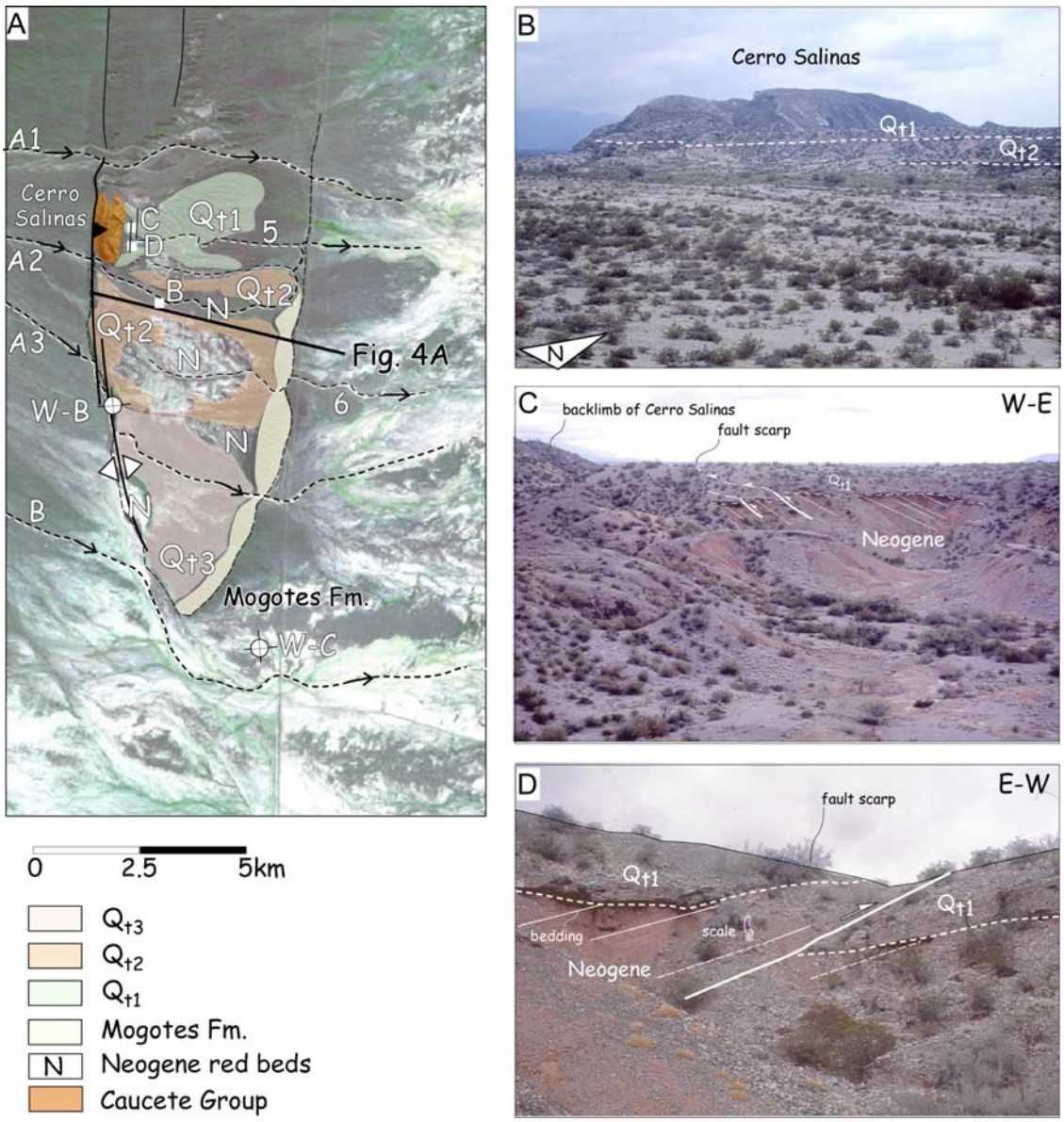

Figure 3. (a) Combined satellite image and geomorphologic map of the Cerro Salinas anticline showing the geometry and extent of folded and thrusted Quaternary terraces (Q_{t1} to Q_{t3}). Small boxes show the position of the photographs in Figures 3b, 3c, and 3d. (b) View of the eastern backlimb of the Cerro Salinas imbricates with Quaternary gravel terraces Q_{t1} and Q_{t2} extending to the east along mainstream A2. (c) W-E view of the thrust faults that are parallel to bedding at the backlimb of the Cerro Salinas. (d) E-W view (opposite than previous picture) of one of these thrusts to show its 12–14 m displacement (the arrow above the thrust is 2.5 m long).

the Neogene and shortening on them continues to the present.

[10] Folded and faulted Quaternary terraces demonstrate that the scale of the active Cerro Salinas anticline is much larger than implied by the relatively limited outcrop belt of the rocks of the Caucete Group (Figures 3c and 3d). We describe in the following section the geomorphology around the Cerro Salinas anticline and its structure through a combination of surface and subsurface data, with emphasis on the surface expression of folding around and south of the Cerro Salinas, which is more clearly expressed than it is to the north of it. The northern continuation of the Cerro Salinas anticline, more than 40 km along strike, is affected by NNE-SSW to N-S trending faults that parallel the Sierra de Pedernal to the west [e.g., *Ramos et al.*, 1997] (Figure 2).

3.1. Geomorphology of the Cerro Salinas Anticline

[11] The geomorphic expression of growing anticlines is recorded in the fluvial system of foreland basins [e.g., *Burbank et al.*, 1996; *Burbank and Anderson*, 2001]. This is noticed in both old Quaternary gravel terraces as have been well preserved in folds developed along both flanks of

the Tianshan Range in China [e.g., *Avouac et al.*, 1993; *Molnar et al.*, 1994; *Hubert-Ferrari et al.*, 2007], as well as in the more recent arrangement of the fluvial network.

3.1.1. Quaternary Alluvial Gravel Terraces

[12] The geomorphic expression of the N-S trending Cerro Salinas anticline is 12–15 km long with a maximum width of 5 km (Figures 2 and 3a). Neogene red beds and overlying Quaternary terraces are uplifted above the modern regional alluvial river system, which flows from the hinterland in the west to the Jocolí foreland basin in the east. Although the anticline is doubly plunging, the anticlinal termination is clear in the south but obscure in the north (Figures 2 and 3a).

[13] Three principal flights of Quaternary terraces (Qt_1 to Qt_3), etched into basement and Neogene cover rocks, outcrop in the region of the Cerro Salinas anticline (Figures 3a and 3b). Gravels overlying the terrace surfaces show a general east to SE direction of paleoflow similar to the modern alluvial drainage network. An individual terrace is marked by an erosional surface into bedrock (a strath) at the base and an overlying cap of gravel with variable thickness.

[14] The uppermost, oldest terrace level (Qt_1) shows the thickest gravel cap with a maximum thickness of 17 m. Its strath is elevated ~22.5 m above the modern river channel (Figure 3). This oldest terrace is mostly preserved in the eastern side of the Cerro Salinas hill where it has been shielded from erosion. The strath of the intermediate terrace level Qt_2 is inset into older terrace Qt_1 and elevated about 15 m above the present river channel. It represents the most continuous surface across the Cerro Salinas anticline and thus used as a marker for recent deformation. Gravel thickness is of few meters. The preserved top of the lowermost terrace level (Qt_3) is elevated about 5 m above the present fluvial network and shows a very discontinuous outcrop along the major fluvial valleys.

[15] Qt_2 terrace is continuous from the forelimb of the Cerro Salinas anticline on the west to its backlimb on the east and covers a large area of the anticline to the south of the Cerro Salinas hill (Figure 3a). A detailed topographic profile was constructed, using GPS, along this transverse to the strike of the Cerro Salinas anticline axial trace along the south side of stream 2; the gradient of which is of about 1° (Figure 4a). At the structural level of Qt_2 the fold geometry is a highly asymmetric west verging anticline with a 130-m western limb that dips 10° to the west, and a >3000-m-wide east flank with a very gentle 1° dip to the east. At the eastern end of Qt_2 a lower terrace, probably corresponding to Qt_3, can be continued for another 2000 m eastward with the same 1°E dip. About 600 m to the west of where more resistant upper Pliocene conglomerates of the Mogotes Formation [*Yrigoyen*, 1993] are exposed in a series of topographic ridges, the inclination of this lower terrace decreases abruptly to only 0.4° to the east (Figure 3a). The present river network also decreases its gradient to 0.4° at about the same position and is inset into white, fine grained playa lake deposits for a distance of ~5 km eastward of the Mogotes Formation hogback (Figure 4a). Both the terrace and modern channels inclinations are consistent with detailed topographic profiles along a number of seismic lines across the study area.

[16] A well-preserved and extensive Quaternary terrace delineates the southern termination of the south plunging Cerro Salinas anticline (Figure 3a). This terrace is lower and less dissected than Qt_2, which implies that it is younger and tentatively correlated with Qt_3. Although difficult to demonstrate on the basis of strath elevation and terrace preservation, a younger age for this terrace would be consistent with the younger growth of the Cerro Salinas anticline toward the south.

[17] Three west directed thrust faults cut terraces Qt_1 and Qt_2 in the backlimb of the Cerro Salinas anticline (Figures 3c and 3d). These faults are east dipping and parallel to the Neogene bedding. Displacement along fault planes is as large as ~10–14 m (Figure 3d). These faults are concentrated in the eastern side of the Cerro Salinas hill and die out to the south, as they do not cut the well-preserved strath at the base of Qt_2 along the south side of stream 2 (Figure 3a). Scarp heights across the faults are several meters high and display relatively straight traces.

[18] Similar N-S trending scarps have been documented along the backlimb of other thrust sheets in the Eastern Precordillera along the Sierra de Pedernal, Sierra de Zonda and Sierra Villicum [e.g., *Uliarte et al.*, 1987, *Martos*, 1993, 1995; *Krugh*, 2003; *Meigs et al.*, 2007] (Figures 1 and 2). The fact that these faults are parallel to bedding in Neogene bedrock indicates they are flexural slip faults caused by folding [*Yeats*, 1986; *Meyer et al.*, 1998; *Meigs et al.*, 2007].

3.1.2. Drainage System Across the Anticline

[19] The drainage system along the front of the Eastern Precordillera in the study area can be subdivided into three main reaches from upstream to downstream. The rivers generally have their headwaters to the west of both Sierra de Pedernal and Sierra de las Peñas and cross the ranges in narrow, steep-sided gorges (Figure 2). Well-developed alluvial fans form at the outlet of these gorges. Primary streams emerging from the range front (labels A and B in Figure 2) branch to the east into multiple channels delineating the active alluvial fans. Fan surface slope decreases from depositional angles of about 2–3° in the proximal parts to ~1° in distal areas across the Cerro Salinas anticline. These secondary streams gradually pass into playa lakes in the foreland to the east, which have depositional slopes of ~0.4° or less.

[20] All the major channels cross the southern termination of the Sierra de Pedernal and the Cerro Salinas anticline as they flow eastward to the modern foreland (Figure 2). Primary stream A flows through a water gap at the southern end of the Sierra de Pedernal and continues to the east as three secondary streams (A1 to A3 in Figure 3a). Secondary streams A1 and A2 cut relatively straight across the Cerro Salinas anticline, to the north and south of the Cerro Salinas hill, respectively. Secondary stream A3, in contrast, is deflected about 2 km to the south along the western surface expression of the Cerro Salinas anticline before crossing it (Figure 3a). A second primary stream, stream B to the south (Figure 2), flows in a structural and topographic gap between the Sierra de Pedernal and the south end of the Sierra de las Peñas. Stream B is diverted to the south around both the southern terminations of the Sierra de Pedernal and the Cerro Salinas (Figure 2). Primary stream B is deflected about 2.5 km southward around the southern termination of the Cerro Salinas anticline (Figure 3a). All streams crossing the Cerro Salinas anticline are incised into bedrock.

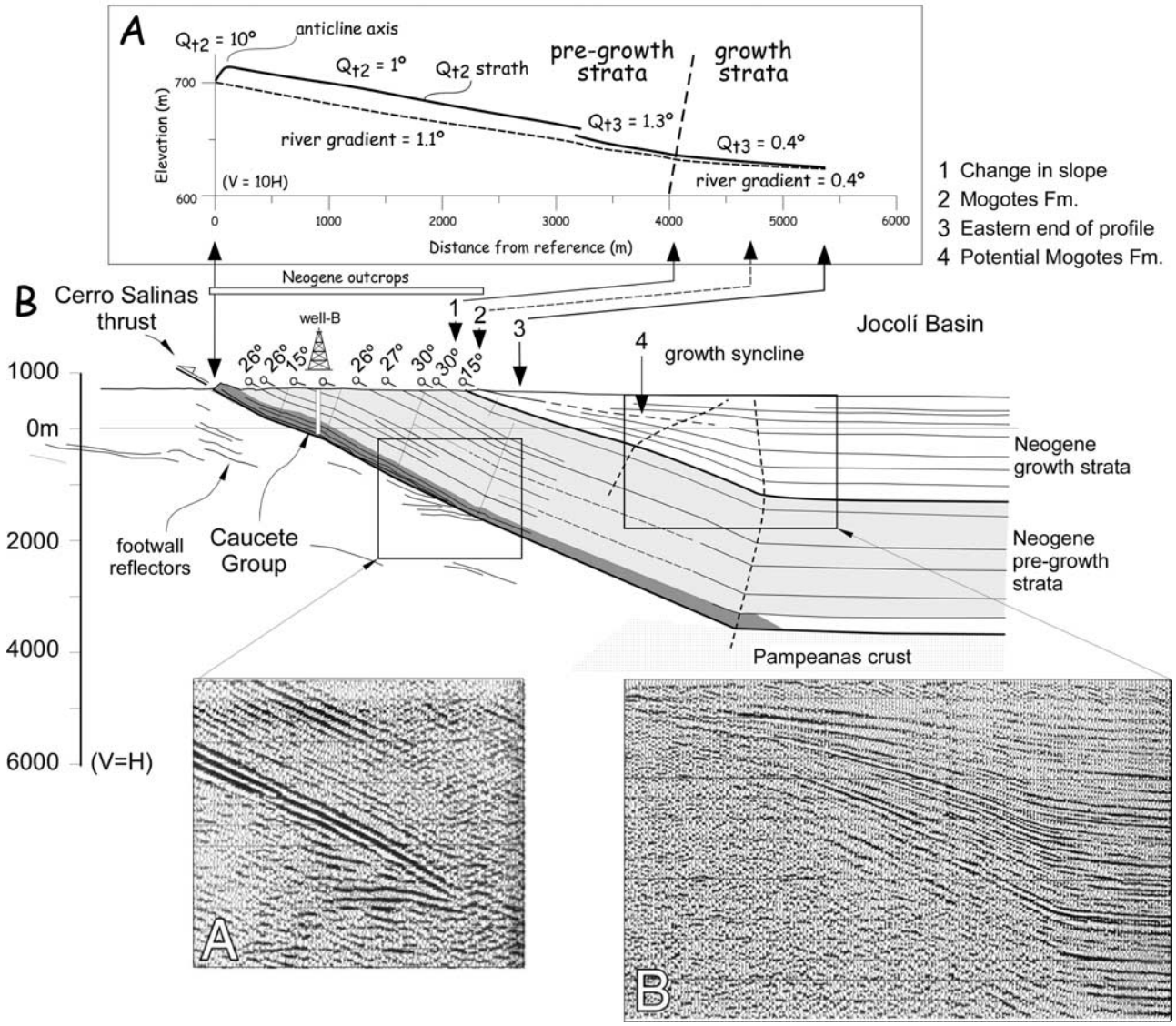

Figure 4. (a) E-W topographic profile of the folded Quaternary terrace Q_{t2} along the south side of the mainstream A2 (see location in Figure 3a). Terrace Q_{t2} shows an asymmetric anticline, which is located on top of the Neogene anticline, although it has a different shape. The abrupt change in slope of both Quaternary terrace and modern river channel has been interpreted as corresponding to the pregrowth and growth strata boundary in the Neogene strata. (b) Combined cross section using field data and line drawing along MCS profile 5367 (see location in Figure 2). The Cerro Salinas thrust separates a hanging wall flat from a footwall ramp. The growth syncline to the east marks the boundary with the undeformed foreland basin.

[21] The uplifted position of the Quaternary gravel terraces and the fact they are folded and thrusted indicate the Cerro Salinas anticline is actively growing. The southward deflections of secondary stream A3 and primary stream B at the western boundary of the Cerro Salinas anticline suggest that emergence of the anticline at the surface due to lateral propagation is ongoing. The location of the change of slope from >1° to ~0.4° of the rivers crossing the Cerro Salinas anticline (stream A2), which occurs to the east of the Mogotes ridge (Figure 4a), and the point at which the primary stream B turns to the east, which occurs south of the Mogotes ridge (Figure 3a), indicate that affect on the surface of the Cerro Salinas anticline is greater than the region of uplifted Quaternary terraces and exposed bedrock. The corresponding decrease of topographic relief, relative terrace age, and structural relief southward along the Cerro Salinas anticline together with the deflection of the southern river channels around the anticline are indicative of active southward propagation of the anticline.

3.2. Structure of the Cerro Salinas Anticline

[22] A number of multichannel seismic lines (MCS) developed by YPF during the early 1980s and three exploratory wells constrain the structure and growth history of the

Cerro Salinas anticline (Figure 2) [*Figueroa and Ferraris*, 1989]. We combine field geology and interpretation of MCS profiles to define the structure across the Cerro Salinas anticline. Two profiles demonstrate that the Cerro Salinas anticline developed in the hanging wall of a thin-skinned thrust ramp and reveal the anticlinal growth history in growth strata: MCS profiles 5367 and 31017 across the central and southern segments of the anticline, respectively (Figure 2). Three exploration wells are incorporated into the sections and interpretations (W-A, W-B, and W-C in Figure 2) [*Figueroa and Ferraris*, 1989]. Exploratory well B is short, located in the crest of the Cerro Salinas anticline has been projected into profile 5367. Exploratory wells A and C have been projected into seismic line 31017 in the hanging wall of the Sierra de las Peñas and in the eastern limb of the Cerro Salinas anticline, respectively.

3.2.1. Central Segment of the Cerro Salinas Anticline Along MCS Profile 5367

[23] MCS profile 5367 in the central part of the anticline roughly parallels both continuous Neogene strata outcrops along A2 stream channel and the Qt_2 profile (Figure 4a). The Cerro Salinas hill constitutes the western end of this cross section (Figure 4b). The hill consists of a stack of imbricated thrust sheets involving Proterozoic strata and has a maximum structural thickness of about 500 m. Individual east dipping thrusts separating the tectonic slices imbricates from the main basal thrust (SW segment of thrusts) to the NE where is covered by Neogene red beds [*Cominguez and Ramos*, 1991]. This internal arrangement is similar to the observed structure of Sierra de Pedernal, Sierra de Zonda and Sierra Villicum (Figure 1).

[24] In the Cerro Salinas, Neogene red beds onlap the stack of Paleozoic thrust imbricates indicating that thrusts were emplaced and formed a moderate paleotopography, with a maximum relief of a few hundred meters, prior to the onset of deposition in the Neogene Jocolí foreland basin. Two main units comprise the Neogene deposits in the backlimb of the Cerro Salinas anticline. The lower part of the Neogene sequence is ~1700 m thick and is dominated by red shales, fine-grained sandstones and uncommon thin conglomeratic layers corresponding to the Mariño Formation (Figure 4b). Dip of this part of the Neogene succession is relatively constant and to the east (Figure 4b), and changes systematically from a shallow ~15° east dip to a constant dip of ~25° east from west to east, respectively. Above these red beds, a sequence of conglomerates, the Mogotes Formation forms a hogback that outlines the backlimb of the Cerro Salinas anticline on both eastern and southern boundaries (Figure 3a). Mogotes conglomerates dip ~15° east and rest unconformably over the lower Neogene succession.

[25] Field relationships suggest that the Cerro Salinas thrust, the basal thrust of the imbricate system, cuts Neogene deposits in the footwall. There is no west dipping forelimb preserved in the hanging wall of the Cerro Salinas thrust in this transect. The Cerro Salinas thrust can be traced along strike to secondary stream A2 (Figure 3a). South of that point an anticlinal axial trace continues along strike to the south. The Cerro Salinas anticline is asymmetric, with a western limb expressed in both the dips of Neogene strata (45°W) and Quaternary terraces (10°W). These west dipping units are part of the very narrow (~100 m) forelimb. The eastern, backlimb dip is fairly homogeneous.

[26] Structural geometry as revealed by MCS profile 5367 fits well with the structural geometry delineated from field data. The profile shows a well imaged Cerro Salinas thrust and a thick group of hanging wall reflectors that parallel the Cerro Salinas thrust. These reflectors project up dip to the 25° east dipping lower Neogene succession (Figure 4b). Parallel reflectors in the lower Neogene succession indicate that it is part of the pregrowth stratigraphic succession (i.e., there is no thickness change across strike). The parallel geometry of the Cerro Salinas thrust and the Neogene succession above it indicates that the hanging wall corresponds to a flat with a ~25° east dip. Exploratory well B encountered late Cambrian-Early Paleozoic imbricates at a depth of 800 m in the hanging wall of the Cerro Salinas thrust [*Figueroa and Ferraris*, 1989] (Figure 4b). In the footwall of the Cerro Salinas thrust there are a group of short and bright reflectors dipping 18° to the east that are cut by the fault plane. These reflectors are interpreted as part of the footwall ramp in the Neogene strata. The close proximity of the hanging wall flat reflectors and the footwall ramp reflectors supports the interpretation of thin-skinned thrusting for the Cerro Salinas [*Vergés et al.*, 2002]. This east dipping footwall ramp continues to a depth of about 3250 m below sea level (bsl) where it changes to subhorizontal delineating a syncline (Figure 4b). In this syncline the lowermost unit is formed by 2100 m of pregrowth Neogene strata marked by a fairly constant thickness. Above these pregrowth strata are ~1800 m of strata that shows a significant decrease in thickness to the west of the syncline axial surface that separates the backlimb of the Cerro Salinas anticline and the undeformed foreland strata (Figure 4b). This wedge-shaped geometry is characteristic of sediment deposited above a growing syncline (so-called growth strata).

[27] The Cerro Salinas growth syncline shows two upward convergent axial surfaces (Figure 4b). We employ the terminology of growth folding of *Suppe et al.* [1992] to describe the nature of these two axial traces. An axial trace marking a change from constant to decreasing thickness is termed a growth axial surface. No change in stratal thickness, in contrast, is characteristic of an active axial surface. A triangular region, a growth triangle, is described by the two axial traces. The eastern of the two axial traces separates flat-lying Neogene strata from east dipping strata in both the pregrowth and growth stratal packages, neither of which change thickness across the axis. The eastern axis is therefore an active axial trace, which dips steeply toward the west in the pregrowth unit and increases dip to subvertical in the growth strata unit. A second axial surface to the west is apparently restricted to the growth strata and marks a change in dip from moderately to gently east dipping from east to west, respectively. Although the pregrowth unit apparently thins from 2100 m at depth to 1700 m to the west, it is unclear whether this thinning is associated with the growth axis. The growth axial surface, less clearly defined, dips 28° to the west. Growth strata display progressive thinning both within the growth triangle and to the west of the growth axial surface (Figure 4b). These stratal characteristics are typical of combined kink

band migration and limb rotation mechanisms of folding and are discussed in a subsequent section.

[28] The minimum amount of the Cerro Salinas thrust displacement in this transect is 6 km to the well-defined footwall ramp reflectors and 9.5 km to the inferred base of the footwall ramp where it intersects the active axial surface of the growth syncline (Figure 4b). During thrust displacement, strata in the hanging wall experienced a minimum vertical uplift of about 4 km. To the west of Cerro Salinas, Neogene deposits located in the basin between the Cerro Salinas thrust and the Precordillera are relatively undeformed, but the base of the Neogene is located at about 1800 m below the present topography and thus elevated with respect the same contact in the Jocolí Basin to the east (Figure 4b). If we assume that the base of the Neogene deposits was at the same level in hanging wall and footwall before thrusting, we must conclude that the footwall beneath the Cerro Salinas thrust has been uplifted by 2.2 km during shortening. This regional footwall uplift, however, cannot be attributed to the west directed thin-skinned thrusting of the Cerro Salinas thrust and must be related with a deeper thrust in the basement.

3.2.2. Southern Termination of the Cerro Salinas Anticline Along MCS Profile 31017 and Its Associated Growth Strata

[29] MCS profile 31017 crosses the south termination Cerro Salinas and the Sierra de las Peñas front. Both structures are exceptionally well imaged beneath the modern alluvial surface, as is the associated growth syncline to the east (Figure 2). The profile, converted to depth by *Cominguez and Ramos* [1991], imaged the buried geometry of the Cerro Salinas anticline across its south termination (Figure 5). These data, when tied to exploratory well C provides constraints on the timing of Cerro Salinas anticlinal growth.

[30] The Central Precordillera thrust front outcrops along the Sierra de las Peñas above the las Peñas thrust (Figure 5) [*Costa et al.*, 2000]. This emergent thrust is well imaged in the seismic line at depth. It dips an average of 20° to the west or W-SW with a similar disposition of the front southward at the latitude of the city of Mendoza [*Bettini*, 1980]. At the surface, the las Peñas thrust carries highly deformed Tertiary red beds above little deformed Quaternary alluvial gravels outcropping at the las Peñas river outlet (Figure 2). Exploration well A, on the hanging wall of the Sierra de las Peñas, crossed the las Peñas thrust at about 900 m below the surface and more than 2200 m of Tertiary rocks in its footwall. Footwall structure comprises a symmetric anticline (Figure 5). Below these slightly folded Tertiary deposits, a relatively thin Triassic unit constitutes the lower part of the las Peñas footwall section. These Triassic strata correspond to the eastern pinch out of a thicker Triassic basin (the buried Cuyo Basin to the south), which is partly involved in the Precordillera thrusting and exposed in thrust sheets in the Sierra de las Peñas to the west (Figure 2).

[31] The Tertiary deposits in the footwall of the las Peñas thrust constitute a 12- to 13-km-wide basin confined between the Precordillera and the Cerro Salinas (Figure 5). Two small folds showing opposite vergence deform these Tertiary deposits. A western anticline is located beneath the las Peñas thrust whereas the eastern anticline is developed above a detachment thrust in the Cerro Salinas thrust footwall. The base of the Tertiary deposits is located at a depth of 3900 m below the present surface showing a regional dip of about 1°–2° toward the east, dip which increases to about 14° east beneath the Cerro Salinas thrust. This segment of the foreland basin defined the western edge of the Jocolí foreland basin prior to growth and emergence of the Cerro Salinas thrust.

[32] An open fold characterizes the Cerro Salinas anticline on the profile and is about 5 km in width, symmetric, and is in the hanging wall of the east dipping and west directed Cerro Salinas thrust (Figure 5). The Cerro Salinas thrust has a complex geometry changing from dipping 18°–24° east below the Cerro Salinas anticline to 45° east in its deeper segment. The footwall geometry shows a low-angle ramp for the shallower segment of the thrust and a high-angle ramp for its deeper segment. The hanging wall geometry has a flat geometry, except where it cuts the forelimb of the Cerro Salinas anticline. Two east dipping steep thrusts with relatively small displacement complicate the geometry of the Cerro Salinas hanging wall anticline (Figure 5). Although the footwall of the Cerro Salinas thrust is not well imaged in this profile, the flat geometry of its hanging wall fits with a thrust detached below, but parallel to, the base of the Tertiary succession [*Vergés et al.*, 2002].

[33] The Cerro Salinas thrust sheet, including the ~5500-m-thick Neogene succession, defines a monocline in this seismic line. A pregrowth and growth subdivision of the Neogene strata is indicated by thickness variations and reflector geometry between Cerro Salinas and the western edge of the Jocolí Basin (Figure 5). A lower ~2200-m-thick pregrowth unit and an upper ~3300-m-thick growth unit can be differentiated across the east facing monocline. The upper part of the Neogene sequence was crossed by exploratory well C located to the SSE of the south termination of the Cerro Salinas anticline near the small village of El Ramblón (Figure 2). The projection of this well onto the line of the section is not straightforward due to along-strike changes of the structure. We used the syncline axial trace as a frame of reference to project the well parallel to the syncline axial trace onto the profile, because the axial trace is laterally continuous in the field and in the subsurface. Well C perforated 3076 m of Tertiary strata and ended in volcanic ash-rich deposits. These volcanic ashes were interpreted as "Tobas grises superiores" [*Figueroa and Ferraris*, 1989], although there is no direct age control for these in the study area. The projection of the well data into the section indicates that the ash-rich beds are located very close to the contact between the pregrowth and growth units. The pregrowth unit is not exposed in this transect, but correlates with the succession of reddish mudstones and fine-grained sandstones with rare conglomerates exposed at the top of MCS profile 5367 (Figure 4).

[34] The growth syncline on MCS 31017 shows curved-hinge zones and subparallel axial surfaces dipping steeply to the west in the pregrowth unit (Figure 5). In the growth unit, the orientation of the syncline active axial surface is similar to the one in the pregrowth unit. The growth axial surface is gentler in the growth strata (~35°W) than in the pregrowth strata (~62°W) and converges upward with the active axial surface defining a growth triangle. The depositional thinning of the growth strata unit toward the crest of the

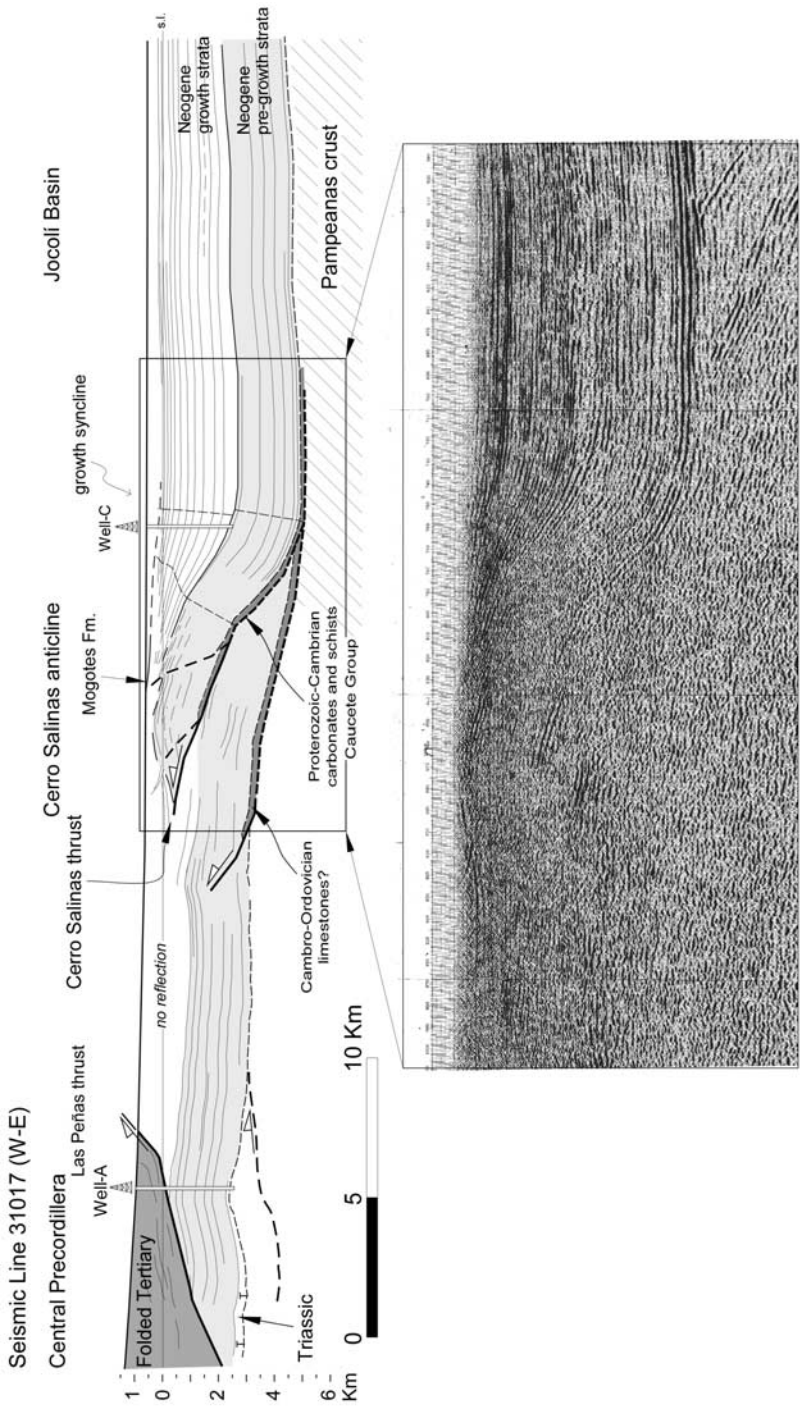

Figure 5. Interpretation based on depth converted MCS profile 31017 crossing the south termination of the Cerro Salinas anticline (see location in Figure 2). We interpret the presence of the Caucete Group located at the basal part of the Cerro Salinas thrust as in MCS profile 5367 in Figure 4b. The west directed thrust in the footwall of the Cerro Salinas thrust is a structure in the Eastern Precordillera.

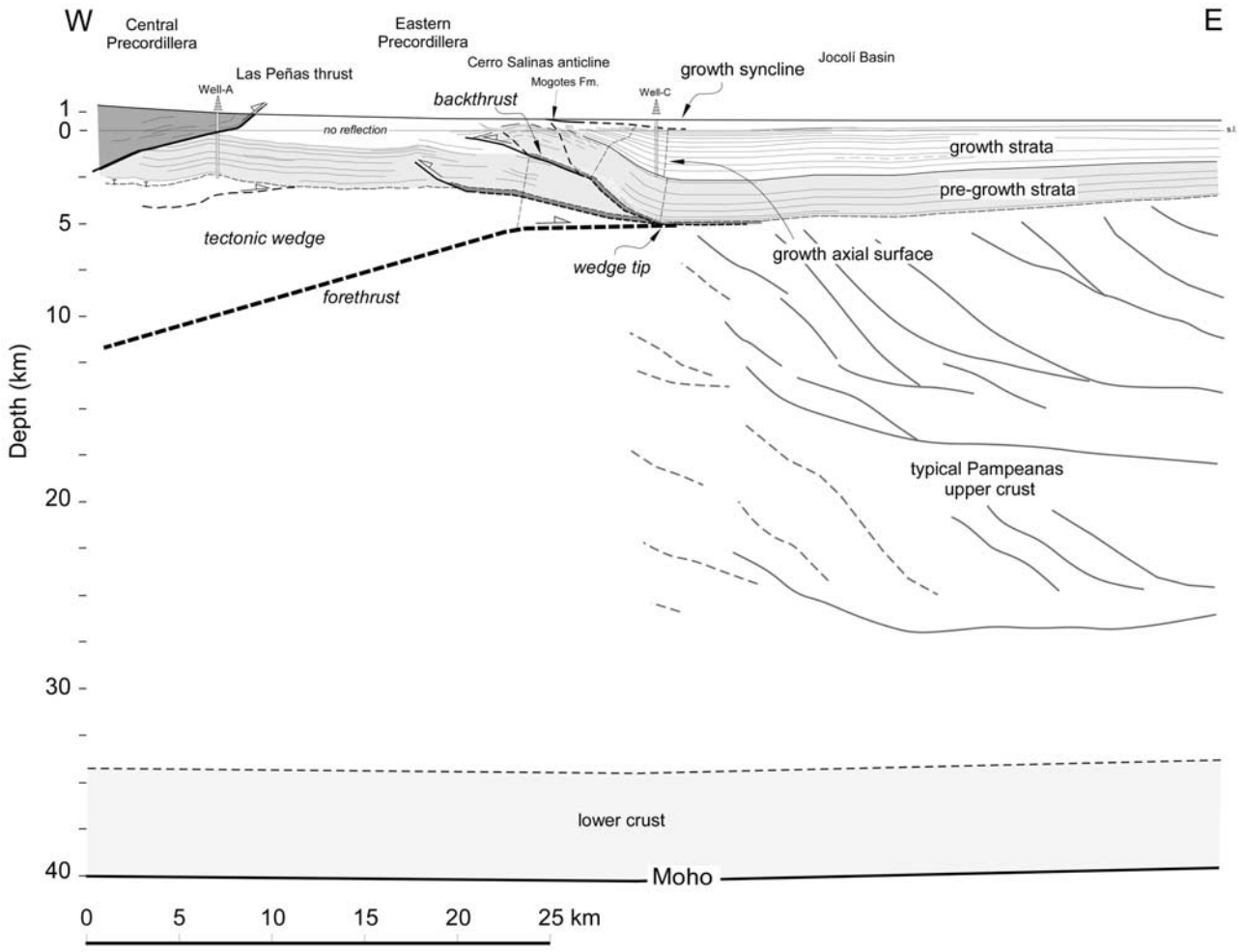

Figure 6. Crustal cross section along MCS profile 31017 to show the tectonic wedge geometry inferred from upper crustal structure. The east directed and low-angle blind fore thrust at depth explains the monocline to the east of the Cerro Salinas thrust. Paleozoic structural grain is depicted beneath the Jocolí Basin and is a widely developed fabric in the crust beneath the Sierras Pampeanas domain.

anticline is progressive in both the growth triangle domain and to the west of the growth axial surface. This is a characteristic also documented across the central segment of the anticline along MCS profile 5367 (Figure 4).

[35] There are an increasing number of both field and subsurface examples of growth synclines that show curved-hinge zones and progressive thinning within the growth triangle [e.g., *Ford et al.*, 1997; *Suppe et al.*, 1997]. Some of these examples have been modeled using wide hinge zones bounded by a pair of axial surfaces separated about few tens to one hundred meters [e.g., *Novoa et al.*, 2000; *Hubbert-Ferrari et al.*, 2005]. In the case of the growth syncline linked to the Cerro Salinas anticline we propose a combined mechanism of growth via limb rotation and kink band migration. The mechanisms operate contemporaneously due to coupled displacement of the Cerro Salinas thrusts footwall monocline growth [e.g., *Marrett and Bentham*, 1997].

[36] Displacement along the Cerro Salinas thrust is about 7–7.5 km whereas the uplift of rocks in the hanging wall above the thrust is of 3.8 km. Part of that uplift is associated with thrust duplication by the Cerro Salinas thrust and part is related to uplift of the footwall monocline.

[37] The base of the Neogene sequence between the Cerro Salinas thrust and the las Peñas thrust is 1.8-km shallower than it is in beneath the undeformed Jocolí foreland basin to the east, similarly to more to the north along MCS profile 5367 (Figure 5). At the scale of the Cerro Salinas anticline, however, the base of the Neogene sequence in the core of the growth syncline is 1.7 km deeper than along MCS profile 5367. Thus the depth to the base of the Neogene beneath the Jocolí basin and the footwall of the Cerro Salinas thrust is 1.9 ± 0.2 km deeper than along the northern profile crossing the center of the anticline (MCS 5367, Figure 4), indicating the southern plunge of the monocline as well.

4. Tectonic Wedge Model for Crustal Structure Beneath the Cerro Salinas

[38] In this section we construct a crustal-scale model that integrates field observations and fault-related fold models to

provide at least a consistent geometry for the proposed structure in an area where no deeper structural constrains are available (Figure 6). Key observations that must be reconciled in this structural model include (1) the west directed Cerro Salinas thrust is thin skinned; (2) the Cerro Salinas thrust soles into a basal detachment in Late Proterozoic-Cambrian strata [*Vergés et al.*, 2002]; (3) the base of the Neogene sequence is ~2 km shallower between to the west of Cerro Salinas than beneath the Jocolí Basin to the east; (4) the east facing Cerro Salinas monocline is defined by the bending of the Neogene succession and Cerro Salinas thrust above a deeper structure that shows ~14° east of forelimb dip; (5) the Neogene succession is composed of pregrowth and growth units that record the growth of the monocline and, to a lesser extent, the Cerro Salinas hanging wall anticline; and (6) the growth unit defines a growth triangle in which the active axial surface coincides with the base of the footwall ramp of the Cerro Salinas thrust.

[39] Our proposed model for the Cerro Salinas at depth consists of a tectonic wedge, defined as by *Shaw et al.* [2005], in which the lower fore thrust is east directed and detached at depth within the basement. The Cerro Salinas thrust is the west directed thin-skinned back thrust. These two conjugate thrusts merge at the tip of the tectonic wedge located at the lower part of the active axial surface of the growing monocline and Cerro Salinas thrust intersection (Figure 6). A change in angle from subhorizontal to 14° east of the base of the Neogene marks the position of the west dipping axial surface that bounds the fore thrust hanging wall ramp to the west. This axial surface is nearly parallel to the active axial surface in the growth syncline about 8.6 km to the east. Forelimb of the wedge-top fold (14° east) below the Cerro Salinas back thrust is used to interpret the angle of the fore thrust at depth from the fold bend fault model described by *Suppe* [1983]. The position of the two axial traces together with the 14° east forelimb dip of the hanging wall fold indicate the fore thrust ramp dips 14° west [*Suppe*, 1983]. Uplift above the crest of the basement wedge explains the ~2 km difference in elevation of the foreland basin strata west of the Cerro Salinas thrust relative to the base of equivalent strata in the Jocolí basin to the east.

[40] Depth converted MCS profile 31017 shows that the crust beneath the detachment in the Late Proterozoic-Cambrian strata is highly reflective basement and has a very distinctive structural fabric [*Cominguez and Ramos*, 1991] (Figure 6). This strongly imbricated crust is defined by two sets of planar to sigmoidal reflectors dipping ~40° toward the east, interpreted as thrusts soling out in a major Proterozoic thrust detachment at ~18 km of depth (17 km bsl) with a second and deeper detachment level imaged at a depth of ~30 km [*Cominguez and Ramos*, 1991]. The detachment level at about 18 km of depth has apparently been reactivated during Tertiary-to-present shortening as indicated by earthquake focal mechanisms that show clusters of earthquakes located at 17–19 km of depth [e.g., *Smalley and Isacks*, 1990; *Smalley et al.*, 1993]. To the east of the Cerro Salinas, however, reactivation of the Paleozoic structural grain is modest and the base of the Neogene succession only shows very subtle folding. To the north, in contrast, thrusting associated with reactivated basement faults deforms the upper crustal rocks as well as the Neogene succession in the Sierra de Pie de Palo [*Ramos and Vujovich*, 2000], and the Bermejo Basin [*Zapata and Allmendinger*, 1996a].

[41] Across the Sierra de Valle Fértil to the east of the Jocolí Basin, two deep seismic reflection profiles show the geometry of the range at depth [*Snyder et al.*, 1990] (Figure 1). The range front thrust, which corresponds to a major early Paleozoic suture zone between the Cuyania terrane and the Gondwana protomargin, is blind along the south line (line 1 in Figure 1) and emergent along the north line (line 2 in Figure 1). In both lines the hanging wall displays a flat fault geometry whereas the footwall is a thrust ramp. This ramp dips about 20–25° to the east and extends to a depth of 9–11 km, which is interpreted as the depth of the detachment [*Snyder et al.*, 1990]. A second detachment level at a depth of 15–20 km is suggested on the basis of fold and fault geometry. The cumulative Cenozoic offset for the Valle Fértil thrust is ~13 km [*Snyder et al.*, 1990].

[42] The crust in this part of the Andes at latitude 32°S is about 40 km thick [*Cominguez and Ramos*, 1991; *Introcaso et al.*, 1992; *Gimenez et al.*, 2000; *Tassara*, 2005]. If these crustal thickness estimates are robust, the fact that the depth distribution of earthquakes is concentrated between 20 and 30 km with a maximum depth at 35–40 km [*Smalley and Isacks*, 1990] suggests that the crust between 30 and 0 km deforms by brittle failure and from 30 km to the Moho by mixed brittle and plastic deformation. The crustal wedge beneath the front of the Precordillera would occur entirely above this transition because it probably extends no deeper than 18 km depth.

5. Timing and Shortening Rate of Cerro Salinas Wedge Emplacement

[43] Growth strata linked to the Cerro Salinas tectonic wedge provide constraints on the timing of basement-involved shortening in the Andean foreland. A key to constraining the onset of basement deformation are the volcanic ash-rich deposits drilled in well C near el Ramblón at a depth of 3076 m interpreted as Tobas grises superiores. These deposits correspond to the youngest ash deposits within this segment of the Andean foreland (Figure 2). The youngest volcanic layers equivalent to the Tobas grises superiores intercalate in the Neogene foreland basin sequences to the north and south of the study area. In the south, a ~1700-m-thick Neogene succession outcrops around the la Pilona anticline and was deposited from 15.7 to 8.4 Ma (see location to the SW of Mendoza in Figure 1) [*Irigoyen et al.*, 2000]. The Tobas de Angostura Formation outcrops in the upper part of the succession and the volcanic ashes there have been dated as 8.64 ± 0.17 Ma [*Irigoyen et al.*, 1999]. In the Albarracín basin, to the west of San Juan, the youngest volcanic ashes are 8.3 ± 0.5Ma [*Vergés et al.*, 2001].

[44] Using these ages for the last ash deposition in the study region, we conclude that the volcanic rocks encountered near the bottom of well C are likely of ~8.5 Ma. Shortening and folding related with the Cerro Salinas tectonic wedge thus initiated after 8.5 Ma (late Tortonian) given that the bottom of well C is near the base of growth strata. An average rate of sediment accumulation of ~0.39 mm/yr (3300 m/8.5 Ma) for the growth unit is implied by this age. Use of growth strata accumulation rates to extrapolate an age for the base of the pregrowth succession

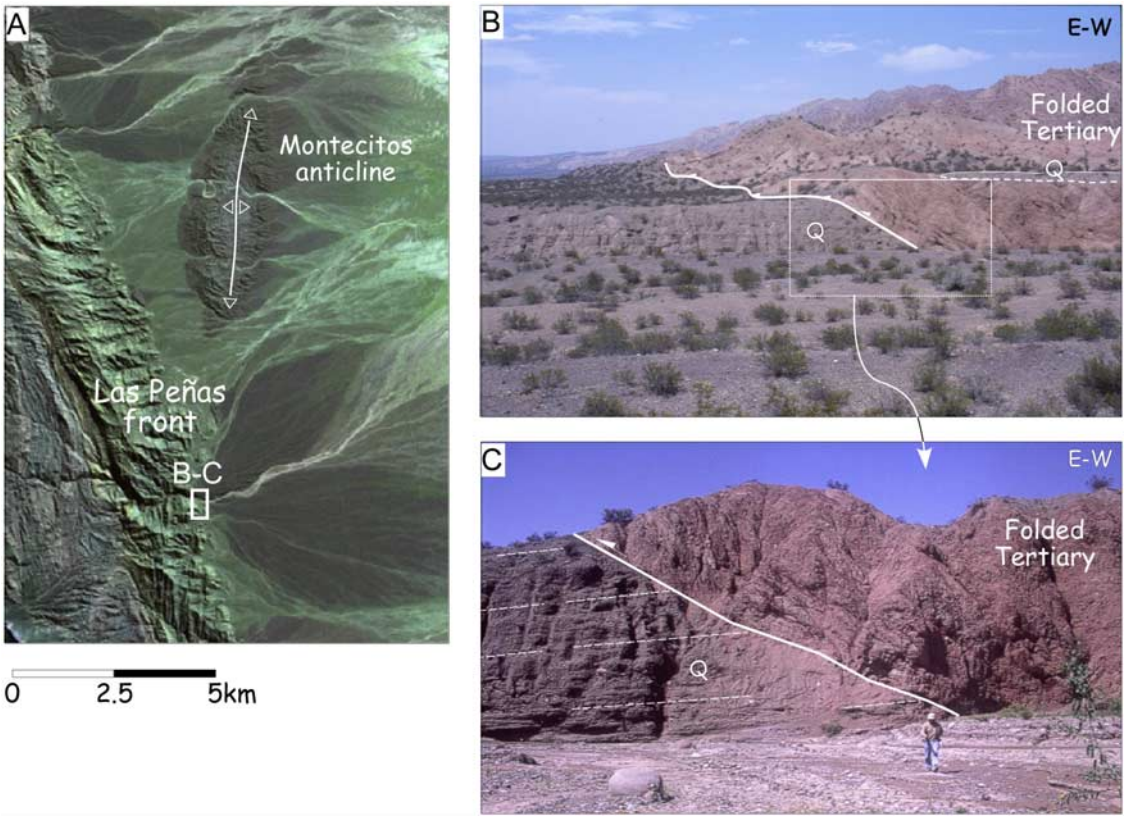

Figure 7. (a) Satellite image showing the Montecitos anticline and the front of the Precordillera at Sierra de las Peñas. Small box shows the position of Figures 7b and 7c. (b) View to the south of the front of the las Peñas from the northern bank of the las Peñas River. The thrust juxtaposes highly folded Tertiary red beds against undeformed Quaternary fluvial deposits. (c) View of the southern bank of the las Peñas River showing the frontal thrust in detail.

is speculative because accumulation rates increase systematically between the early and late stages of foreland infilling (compiled by *Vergés et al.* [2001]) but would give a minimum age of ~14 Ma for the base of the Neogene section. In the La Pilona anticline and the Albarracín basin the base of the Neogene succession is exposed and ranges in age from 16 to 18 Ma, which therefore implies that the base of the Neogene succession in the study area is possibly similar in age.

[45] Assuming an age of ~8.5 Ma for the initiation of the Cerro Salinas tectonic wedge, the rate of displacement along the low-angle basement fore thrust is of about 1.0 mm/yr (8.7 km/8.5 Ma), which is slightly higher than for the Cerro Salinas thin-skinned back thrust along the same MCS profile 31017 (almost 0.9 mm/yr). Horizontal shortening rate is also ~1 mm/yr. The rate of uplift of the Cerro Salinas hanging wall thrust is ~0.45 mm/yr (3.8 km/8.5 Ma).

6. Discussion

6.1. Regional Extent of the Cerro Salinas Deep Structure: Sierra de las Peñas and Sierra de Pie de Palo

[46] We document in this section the lateral extent of the deep structure beneath the Cerro Salinas: to the south along the Montecitos anticline and Sierra de las Peñas and to the north along the Sierra de Pie de Palo.

6.1.1. Montecitos Anticline and the las Peñas Front

[47] The southern continuation of the Cerro Salinas structure is imaged in seismic line 5377 crossing the Montecitos anticline [*Costa et al.*, 2000] (Figure 7a). Montecitos is a 5.5-km-long, 2-km-wide, symmetric, double plunging anticline that shows no trace of thrusting at surface. Growth strata are exposed in both flanks, including the upper Pliocene Mogotes Formation in the upper part of the exposed section [*Costa et al.*, 2000].

[48] The geometry of the Montecitos anticline at depth is not well imaged in any of the seismic lines. However, in MCS profile 5377 (see its position in Figure 2), the Montecitos anticline is located in the hanging wall of a gently east dipping thrust ramp. Neogene strata in the hanging wall show a flat geometry, parallel to the thrust plane, comparable to the ones displayed in MCS profiles 5367 and 31017 across the Cerro Salinas anticline (Figures 4 and 5). Although the seismic line looses its quality up section, the east dipping hanging wall flat appears to connect to the Montecitos anticline near the surface indicating that the anticline formed above and related with the west directed propagation of a blind thrust at depth. Following this interpretation, the Montecitos anticline and its associated Miocene and Pliocene growth strata is likely the along-strike equivalent and southern continuation of the Cerro Salinas anticline. Accordingly, the Montecitos anti-

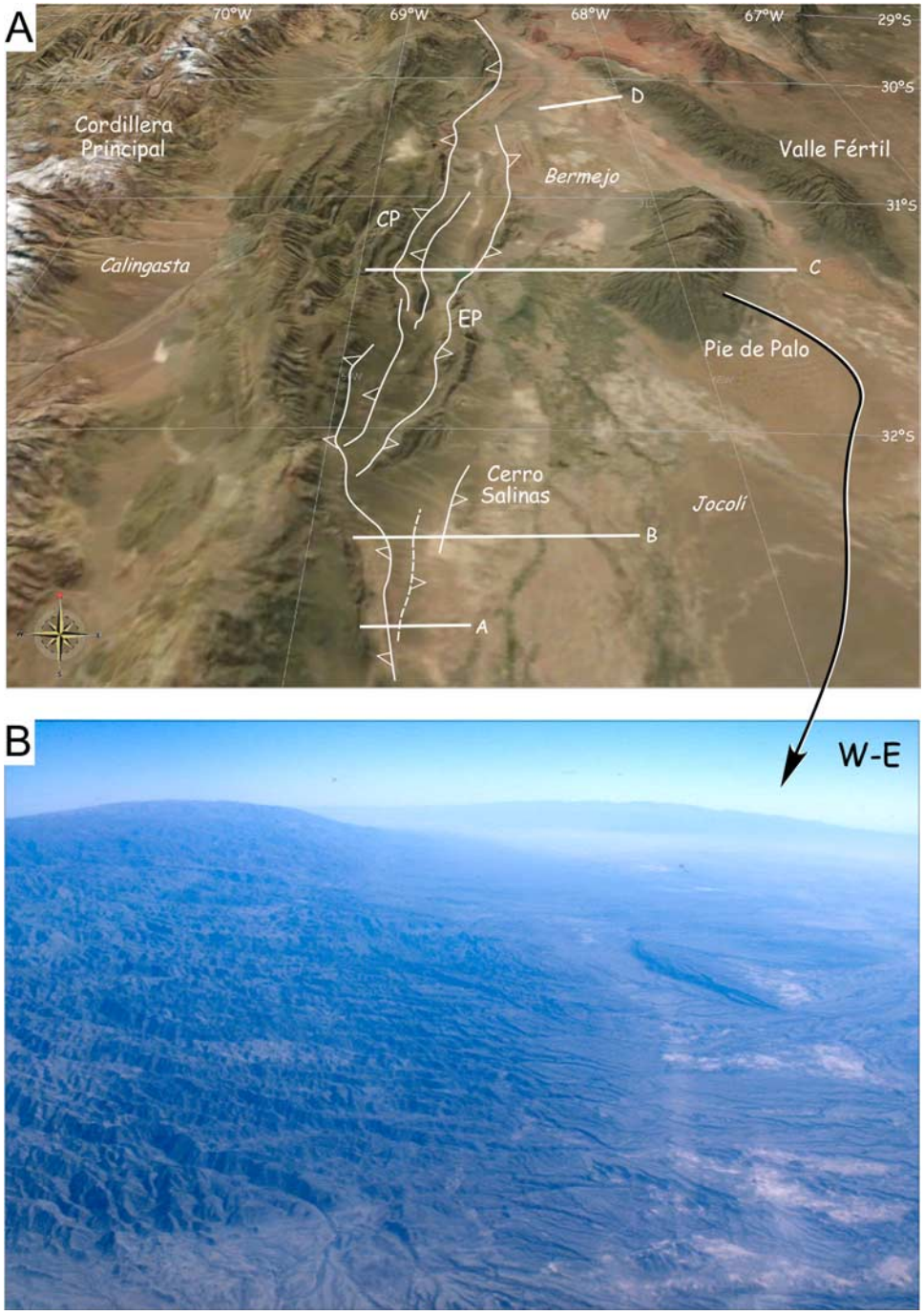

Figure 8. (a) Oblique view of the study area along the front of the Andes at the latitude of the Sierra de Pie de Palo (from NASA WorldWind version 1.3, http://worldwind.arc.nasa.gov). Location of cross sections A–D in Figure 10 are located. (b) Aerial view of the eastern flank of the Sierra de Pie de Palo.

cline is located above the southern continuation of the west directed back thrust that constitutes the upper conjugate thrust of the crustal tectonic wedge defined in the Cerro Salinas transect.

[49] The Montecitos anticline plunges to the SSW beneath the NNW-SSE trending las Peñas frontal thrust [*Costa et al.*, 2000] (Figures 7a and 7b). This thrust front is young and presently active as documented by the array of east directed thrusts cutting recent and very little deformed horizontal Quaternary proximal alluvial terraces at the western boundary of the foreland basin [*Cortés and Costa*, 1996; *Costa et al.*, 2000] (Figure 7c). This Precordillera front overthrusts the southern continuation of the Montecitos anticline and associated west directed blind thrust.

6.1.2. Sierra de Pie de Palo Structure

[50] The Sierra de Pie de Palo is one of the most spectacular uplifted blocks in the Sierras Pampeanas because of its dome geometry and high elevation (3162 m) (Figure 8a). Its structural relief is still more impressive, particularly across the north boundary, where the relief

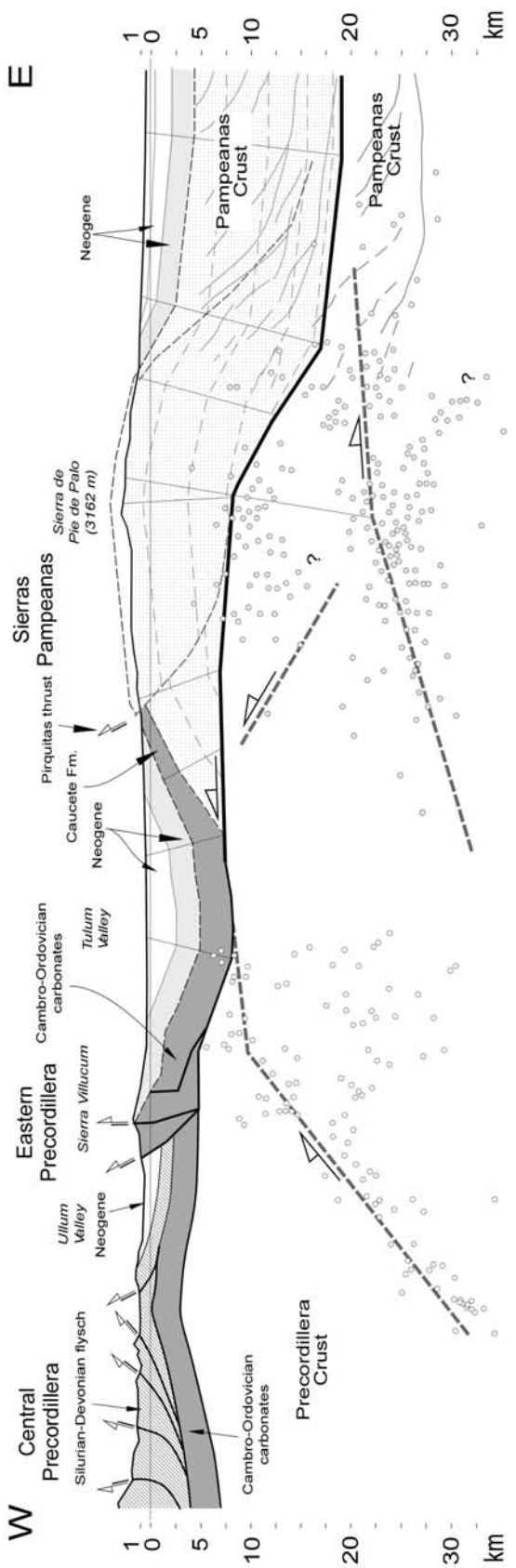

Figure 9. Cross section across Sierra de Pie de Palo based on the work by *von Gosen* [1992], *Ramos et al.* [2002], and *Meigs et al.* [2007]. The seismicity beneath the Precordillera and Pie de Palo is from *Smalley et al.* [1993] and *Ramos et al.* [2002], respectively.

between the top of the sierra and the bottom of the Bermejo foreland basin is more than 10 km [e.g., *Zapata and Allmendinger*, 1996b; *Zapata*, 1997; *Ramos and Vujovich*, 2000]. We discuss a regional section from the front of the Central Precordillera along the San Juan River to the eastern side of the Sierra de Pie de Palo in order to compare the crustal structure of the Eastern Precordillera in the north with the crustal structure to the south across Cerro Salinas. Although the cross section that parallels the San Juan River is well exposed, it is not constrained with reflection seismic data. The cross section in this paper was developed from new field data, existing maps, and reinterpretation of previously published cross sections [*von Gosen*, 1992; *Ramos and Vujovich*, 2000; *Vergés et al.*, 2001; *Ramos et al.*, 2002; *Meigs et al.*, 2007] (Figure 9).

[51] The Central Precordillera consists of an imbricate thrust system that detaches at Silurian-lower Devonian rocks and at a deeper level along the base of the Cambro-Ordovician limestones [*von Gosen*, 1992; *Ragona et al.*, 1995; *Ramos and Vujovich*, 2000] (Figure 9). Near the front of the Precordillera thrust system the Silurian-lower Devonian detachment is located at about 4 km below sea level [*Vergés et al.*, 2001]. The front of the Central Precordillera is represented by a hanging wall anticline cored by Devonian turbidites. The forelimb of the anticline is unconformably covered by the Neogene succession of the Ullum Basin. Several hundreds of meters of Quaternary alluvial infill were drilled by water wells in the center of the Ullum basin above the Neogene (see section of *Colombo et al.* [2000]). The Sierra de Villicum at the eastern side of the Ullum Basin consists of a Paleozoic imbricate thrust system duplicating Cambro-Ordovician limestones that is reactivated and cuts Neogene red beds. Its basal thrust places lower Paleozoic strata in thrust contact with the Neogene sequence of the Ullum Basin. The west directed thrust on the west side of the Sierra de Villicum has been interpreted as an east dipping thrust that roots into the basement [e.g., *Ramos and Vujovich*, 2000; *Cristallini and Ramos*, 2000; *Siame et al.*, 2002]. Bedding in the Paleozoic sequence and the thrust fault have the same dip, which strongly suggests that the thrust system is thin skinned and detached near the base of the Cambro-Ordovician strata [e.g., *Krugh*, 2003; *Meigs et al.*, 2007].

[52] Microseismicity recorded beneath the Sierra de Villicum [*Regnier et al.*, 1992; *Smalley et al.*, 1993] suggests active faulting between 5 and 35 km at depth with a principal plane striking N45°E and dipping about 35°NW. Focal mechanisms indicate active reverse faulting [*Kadinsky-Cade et al.*, 1985; *Smalley et al.*, 1993]. The fault plane has been projected onto the cross section as described by *Meigs et al.* [2007] (Figure 9). Field observations show that the Sierra de Villicum thrust sheet, like the Cerro Salinas thrust sheet, is refolded by an east facing monocline, which is interpreted to reflect the forelimb of an east directed basement wedge at depth. Slip transfer from the basement fault to one or several of the faults within the Villicum thrust system accommodates emplacement of the wedge to the east. The relation between the basement thrust, the Sierra de Villicum thrust system, and surface ruptures associated with the 1944 San Juan earthquake are described by *Krugh* [2003] and *Meigs et al.* [2007]. A recent analysis recalculated the focal mechanisms for the 1944 San Juan earthquake as well as for the one in 1952, concluding that these earthquakes occurred at depths of 11 and 12 km, respectively [*Alvarado and Beck*, 2006].

[53] Sierra de Pie de Palo, to the east of the Sierra de Villicum, is a Proterozoic- and Paleozoic-cored massif that requires a different interpretation of crustal structure [e.g., *Cristallini et al.*, 2004]. The Sierra de Pie de Palo shows a rounded topography exposing a well-preserved regional pre-Neogene peneplain at the top of basement. Its shallow structure corresponds to an antiformal culmination that plunges north and south. The dome is slightly asymmetric with a shorter and steeper east flank (Figures 8a and 8b). Tertiary basins onlap both the east and west sides of the sierra. Although not directly constrained by subsurface data, the base of the Neogene in both basins is at a similar depth. Key observations and assumptions required to define the deep structure of the Sierra de Pie de Palo therefore include (1) the sierra is almost symmetric with very long and gentle flanks; (2) Neogene basins flank the sierra in east and west; (3) there is no major thrust reaching the surface on either flank and, if the sierra formed above a thrust, it must be blind [*Ramos and Vujovich*, 2000]; (4) the structural relief of about 10 km, observed across its northern termination, corresponds to the thickness of the hanging wall above the blind thrust; (5) the pre-Neogene peneplain as well as the distribution of detailed microseismicity recorded after the Caucete 1977 event constrain the thrust geometry at depth (based on work by *Ramos and Vujovich* [2000]); and (6) the inherited west directed structural grain that characterizes the Proterozoic middle crustal levels of the Western Sierras Pampeanas controls the active thrusts [e.g., *Cominguez and Ramos*, 1991; *Zapata and Allmendinger*, 1996b; *Zapata*, 1998].

[54] A fault bend fold model [*Suppe*, 1983] is used to define the geometry of the Pie de Palo thrust at depth (Figure 6). A good fit with shallow structure is accomplished by using a long thrust ramp with sigmoidal geometry that has a low angle in its lower and upper segments and higher angle in the central segment. This west directed thrust ramp would sole out to the east at ~19 km of depth. The ramp geometry fits the geometry of the Paleozoic imbricate thrusts observed in MCS profile 31017 as well [*Cominguez and Ramos*, 1991]. Given the location and orientation of proposed thrust ramp at depth, the hanging wall is about 11 km thick beneath the Pie de Palo culmination and is consistent with the maximum structural relief across the northern end of the sierra. Thrust displacement is ~30 km and the thrust tip is interpreted to connect to the Villicum thrust system beneath the Tulum Basin (Figure 9). The transfer of such a large amount of shortening into the thin-skinned Villicum basal thrust implies a greater amount of shortening in the Sierra de Villicum than is implied in our section. If the onset of thrusting in the Neogene occurred at ~8.5 Ma as it did at Cerro Salinas, a 3.5 mm/yr of displacement along the Pie de Palo thrust fault is implied. This shortening rate is consistent with the shortening estimates of 2.6–4.6 mm/yr for the Sierra de Villicum basement monocline [*Siame et al.*, 2005; *Meigs et al.*, 2007], with the present GPS-derived velocities calculated between the Eastern Precordillera and Sierra de Pie de Palo [*Brooks et al.*, 2003] but are higher, although of the same order of magnitude, than calculated shortening rates for last

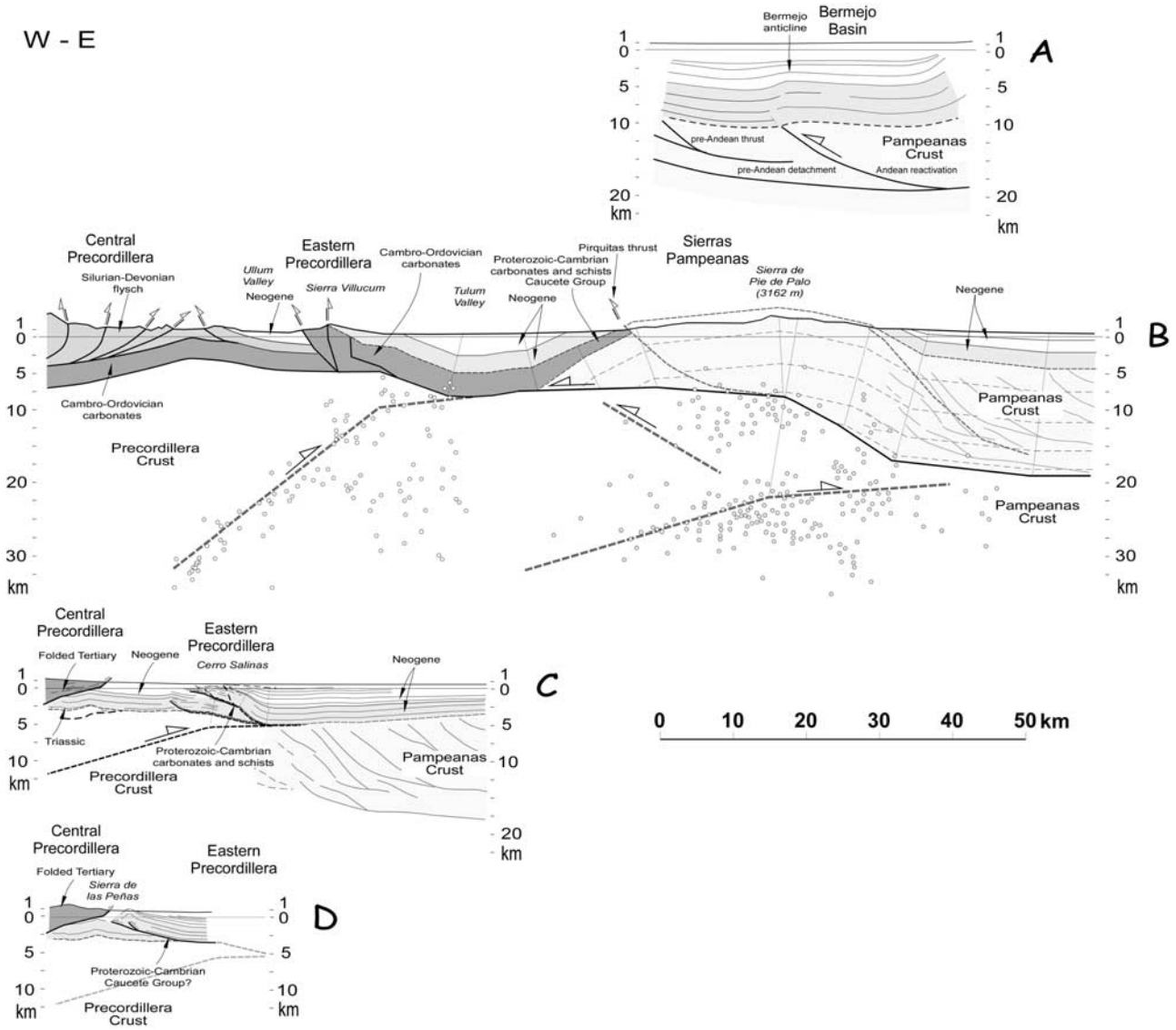

Figure 10. Four schematic crustal cross sections showing the relationships as well as their variation between the opposed thrust systems along the N-S strike of the principal structures. These transects are located in (a) the front of the Sierra de Valle Fértil across the Bermejo Basin (section A along seismic line 9051 described by *Zapata* [1998]), (b) the Sierra de Pie de Palo, (c) the Cerro Salinas, and (d) the Sierra de las Peñas.

~20 kyr using Quaternary faulted deposits nearby the Villicum front [*Siame et al.*, 2002]. If the Pie de Palo thrust is a reactivation of an inherited thrust, this rate is a maximum given that an unknown amount of the 30 km displacement may have accumulated during Paleozoic shortening.

6.2. Precordillera and Sierras Pampeanas Interplay

[55] The interactions between the Precordillera and the Sierras Pampeanas in the study region have been discussed previously [e.g., *Jordan and Allmendinger*, 1986; *Figueroa and Ferraris*, 1989; *Cominguez and Ramos*, 1991; *Ramos et al.*, 2002; *Cristallini et al.*, 2004] and are revised in the light of the new data presented in this paper. Our model for the crustal structure is in agreement with previous interpretations at the scale of the frontal Andes, models which involve opposing thrust ramps detaching at different crustal levels [e.g., *Smalley et al.*, 1993; *Allmendinger and Zapata*, 1996]. Four different schematic cross sections illustrate the proposed structure along Andean thrust front in the boundary region between the Precordillera and the Western Sierras Pampeanas (Figure 10). These sections indicate that the regional structural style is characterized by thin-skinned thrusting in the Eastern Precordillera that is the surface manifestation of basement thrust and tectonic wedge emplacement at depth.

[56] In the north at 30°19′S, a transect across the Bermejo Basin based on good seismic images permitted the geometry of the thrust system to the north of the Sierra de Pie de Palo to be characterized in detail (Figure 10a). This section, from *Zapata* [1998], shows an incipient west directed structure located at a depth of about 18 km, which deforms Late Proterozoic and Lower Paleozoic rocks as well as the Neogene foreland strata. This structure cuts through 8–

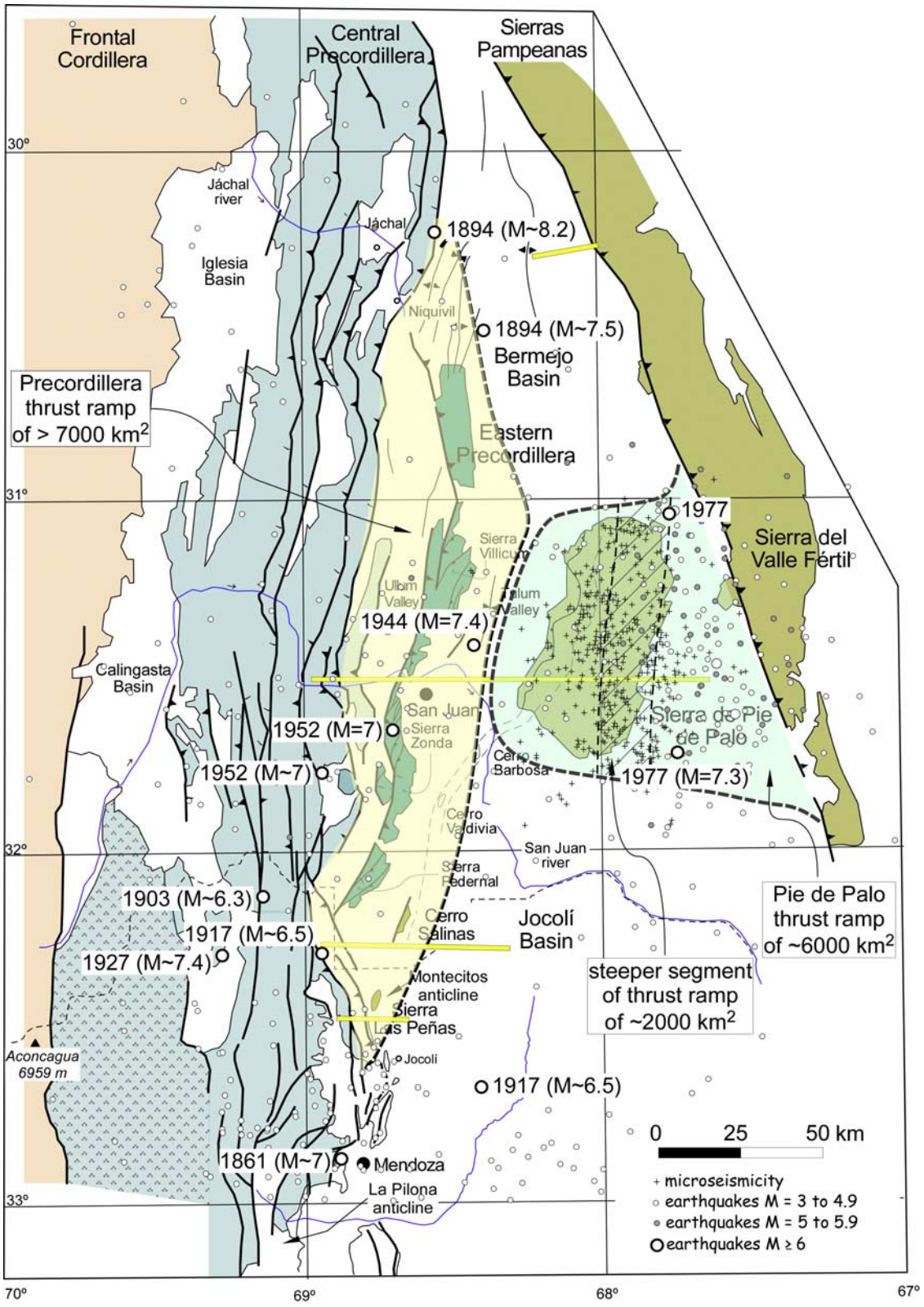

Figure 11. Tectonic map of the study region combined with focal mechanisms for recent earthquakes (NEIC from USGS using USGS/NEIC data from 1973 to Present; http://earthquake.usgs.gov/regional/neic). Historical large earthquakes are also plotted. The maximum extent of the proposed east directed blind thrust beneath the Eastern Precordillera as well as of the west directed blind thrust beneath the Sierra de Pie de Palo are represented and limited by thick dashed lines (tip line of the top of thrust ramps at depth).

9 km of pre-Neogene rocks and corresponds to the northern continuation of the Sierra de Pie de Palo. It is inferred to represent a reactivation of an older structural grain.

[57] At the latitude of Sierra de Pie de Palo (31°31′S) the east directed wedge fore thrust beneath Sierra de Villicum merges upward with the detachment at the base of the Late Proterozoic-Cambrian limestones but displays little displacement (Figure 10b). The Sierra de Pie de Palo uplift, in contrast, is primarily produced by the west directed tectonic duplication of the uppermost ~11-km-thick imbricated basement rocks. In detail, the Pie de Palo is inferred to be underlain by an east dipping ramp that soles out at ~19 km of depth and merges upward with the shallower detachment at the base of the Late Proterozoic-Cambrian limestones. The ~30 km of displacement to the west is transferred in this model to the thin-skinned Sierra de Villicum thrust system.

[58] Along strike to the south, structure beneath the Cerro Salinas (32°14′S) also consists of a tectonic wedge deduced from the uplift of a large portion of the foreland in the footwall of the active Precordilleran thrust front (Figure 10c). The west dipping blind fore thrust, which dips 14° west, merges upward with a regional detachment level along the base of the Late Proterozoic-Cambrian strata of the Caucete Group. At the wedge tip, an east dipping back thrust emplaces the tectonic slices of the Caucete Group over Neogene strata. An incipient anticline in the footwall of the Cerro Salinas thrust might represent the southern end of the Eastern Precordillera ranges. Toward the east of the section, the Sierra de Valle Fértil detaches at mid crustal levels along two detachments at about 9–11 km and 15–20 km at depth.

[59] Near the southern termination of the Eastern Precordillera at 32°25′S, the tectonic wedge model is still valid, but the west directed back thrust and associated Montecitos anticline are cut by the active thin-skinned thrust front of the Central Precordillera at the Sierra de las Peñas (Figure 10d). To the east, the Sierra de Valle Fértil thrust has less displacement as suggested by the southward lowering of topographic relief.

[60] Two major blind and opposed crustal ramps corresponding to the fore thrust of the tectonic wedge in the west and to the west directed Pie de Palo thrust to the east dominate the crustal structure in the boundary region between the thin-skinned Precordillera and thick-skinned Sierras Pampeanas structural provinces. The fore thrust ramp is apparently continuous along the length of the Eastern Precordillera. An area of ~7000 km^2 for this inferred ramp is estimated from the length of the tip line along strike and the downdip limit of the ramp at depth below the Central Precordillera (Figure 11). The westward extent of the proposed east directed blind fore thrust beneath the Ullum Basin and Eastern Precordillera is unknown. Thrust ramps cutting down a large portion of the crust or even the entire crust are supported by regional cross sections [*Ramos et al.*, 2004] and by deep seismic lines across the northernmost Andes in Argentina where a crustal ramp is interpreted to extend into the lower crust [*Allmendinger and Zapata*, 2000]. Post-late Neogene uplift along the San Juan River of ~1500 m since 7.1 Ma with an average rate of 0.22 mm/yr [*Vergés et al.*, 2001] implies that the fore thrust ramp may continue at depth beneath the Central Precordillera (Figure 11). The Pie de Palo west directed blind back thrust is also large and covers a total area of about 6000 km^2. Roughly 33% of that area (2000 km^2) is accounted for by the steep segment of the ramp below the eastern flank of the sierra (Figure 11).

6.3. Precordillera-Sierras Pampeanas Crustal Boundary and Its Seismogenic Implications

[61] The boundary between the Precordillera and the Sierras Pampeanas is dominated by blind thrust faults that likely extend to depth of 20 km or more and which are capable of producing large earthquakes. Historic earthquakes in the study region, however, produced minor, relatively small surface ruptures on secondary faults [*Meigs et al.*, 2007]. Within the study region, most of these surface ruptures are interpreted as flexural slip faults. Bedding parallel flexural slip formed by both coseismic and postseismic motion as documented in the La Laja area where 30 cm of this movement was produced along a period of weeks after the main earthquake [*Castellanos*, 1944; *Groeber*, 1944]. Surface deformation is apparently dominated by folding [*Kadinsky-Cade et al.*, 1985; *Krugh*, 2003; *Meigs et al.*, 2007] similar to other well-documented blind thrust earthquakes such as those in the Los Angeles Basin [e.g., *Yeats and Huftile*, 1995; *Shaw and Suppe*, 1996; *Pratt et al.*, 2002].

[62] We thus propose that historical earthquakes devastating large regions of the study area occurred by the coseismic slip on these blind thrusts by the rupture of relatively large fault segments in the basement. Using the size of these events, it is possible to calculate the area of the rupture of the faults using empirical relationships for thrusts developed by *Wells and Coppersmith* [1994]. The 1944 La Laja event with M_w = 7.0 [*Alvarado and Beck*, 2006] and thus the area of rupture is about 900 km^2. The 1952 seismic event to the south of the city of San Juan with M = 6.8 [*Alvarado and Beck*, 2006] possibly ruptured about 550 km^2. These rupture areas at depth are compatible with the thrust fault areas of the west dipping fore thrust. The relatively small area of these ruptures compared with the assumed total area for this ramp implies either (1) that the ramp is not a continuous plane and consists of discrete segments or (2) that the seismic events ruptured small patches or segments of a single continuous thrust ramp. Although the relatively scattered distribution of deep seismicity supports the model of discrete thrust ramps, which is also implied by the complex tectonic grain inherited from the Paleozoic deformation, a very large earthquake with a magnitude of about 7.7 would result from rupturing a single ramp along the length of the Eastern Precordillera. The 1977 Caucete event (M = 7.4 [*Kadinsky-Cade et al.*, 1985]) requires a rupture area of about 2600 km^2, which fits well with the proposed area for the steeper central segment of the west directed thrust ramp located beneath the eastern side of the Sierra de Pie de Palo (Figure 11). This result also agrees reasonably well with the observed area distribution of the aftershocks documented after the 1977 Caucete earthquake [*Smalley et al.*, 1993].

[63] Combining long-term fault displacement rates, potential rupture areas, and the assumption that most of this displacement is released during large earthquakes it is possible to calculate earthquake recurrence intervals [*Shaw and Suppe*, 1996]. Because our long-term fault slip rates are

small, the estimated recurrence intervals are relatively long. The east verging blind fore thrust rate of displacement at Cerro Salinas thrust is 1 mm/yr, which suggests that recurrence interval ranges from about 1100 yr for earthquakes of $M = 7$ to about 2000 years for $M = 7.4$. For the Sierra de Pie de Palo thrust, where long-term rates are of 3.5 mm/yr, the recurrence interval for a characteristic $M = 7.4$ earthquake like the Caucete event in 1977 is of less than 600 years if we assume that deformation started at 8.5 Ma like in the Cerro Salinas example (30 km/8.5 Ma). If that rate is too high because some of the shortening accumulated in the Paleozoic, the recurrence interval would be longer and more consistent with the ~1000 year recurrence interval estimated by *Kadinsky-Cade et al.* [1985].

[64] In conclusion, the large blind crustal ramps documented in this work represent a potential source of seismic risk capable of generating large earthquakes, which will damage the cities of San Juan and Mendoza as they have in the past. The low rates of tectonic shortening accommodated by these structures in the last 8.5 Myr indicate that relatively long intervals (thousands of years) separate seismic events. This inference is supported by one of the few trench studies of an active secondary fault in the Eastern Precordillera, the Marquezado Fault to the north of Cerro Salinas, in the backlimb of the west directed Zonda thrust, which shows that the last faulting event occurred before 2505 ± 160 years, using ^{14}C technique [*INPRES*, 1982].

7. Conclusions

[65] Integrated surface, subsurface, and geomorphic studies are required to constrain the tectonic structure of active mountain fronts where blind thrust faulting predominates, such as is the case of the 200-km-long front of the Andes between the densely populated cities of San Juan and Mendoza in Argentina. To define the deep structure along the boundary region between the Precordillera and the Sierras Pampeanas thick-skinned province, we combined surficial studies with interpretation of industry seismic lines to construct an integrated and quantified model of crustal architecture. This method has been applied to the Cerro Salinas at the south termination of the Eastern Precordillera and then extended to the north and south to characterize the regional structure and its seismogenic potential.

[66] The Cerro Salinas surficial structure consists of an anticline defined by both Neogene red beds and folded Quaternary fluvial terraces developed on the hanging wall of the west directed Cerro Salinas thrust. This thin-skinned thrust detached at the base of the 500-m-thick imbricated Proterozoic carbonates and shales of the Cerro Salinas hill. The recent uplift along this fold is recorded by a set of uplifted, folded and thrusted Quaternary fluvial terraces (Q_{t1} to Q_{t3}) and by the deflection of the modern fluvial network flowing across the anticline. Displacement of the Cerro Salinas thrust is of 7–9 km. The Cerro Salinas thrust and the western sector of the Jocolí Basin Neogene succession is folded by an east directed monocline, which is well imaged in the southern termination of the Cerro Salinas anticline along MCS profile 31017.

[67] A 5.5-km-thick Neogene sequence folded by the monocline consists of about 2.2 km of pregrowth and 3.3 km of growth strata. The growth syncline shows a growth triangle with the active axial surface pinned in the syncline axis and a growth axial surface located in the backlimb of the Cerro Salinas anticline. Growth strata thin in both the growth triangle and toward the crest of the anticline suggesting a hybrid kinematic fold evolution characterized by both kink band migration and limb rotation.

[68] The deep structure beneath the Cerro Salinas monocline is interpreted as a tectonic wedge delineated at depth by a low-angle, east directed blind fore thrust ramp with a dip of 14°. This blind fore thrust connects at its tip with the Cerro Salinas thrust, which constitutes the back thrust of the tectonic wedge. Uplift and frontal folding of the fore thrust produced the 2 km regional uplift observed of the hanging wall to the west of the Cerro Salinas.

[69] An age of ~8.5 Ma for the initiation of the Cerro Salinas tectonic wedge has been determined with the regional dating of the Tobas grises superiores encountered near the boundary between the pregrowth and growth strata units. This age indicates that rates of shortening are relatively low (1 mm/yr) for the Cerro Salinas structure. The rate of uplift of the hanging wall of the Cerro Salinas thrust integrating back thrust thrust displacement and monoclinal uplift above the fore thrust of ~0.45 mm/yr.

[70] The Montecitos anticline represents the southern continuation of the Cerro Salinas anticline, which is overthrust by the Central Precordillera at the active las Peñas thrust front. The northern continuation of the Eastern Precordillera tectonic wedge is located beneath the Eastern Precordillera at the Sierra de Villicum. The Sierra de Pie de Palo formed above a thick-skinned west directed blind thrust that detaches at a depth of 17 km in an intracrustal detachment. This west directed back thrust has a total displacement of 30 km that is transferred updip to a thin-skinned thrust along the basal décollement of the Eastern Precordillera.

[71] The potential seismic hazard of the blind thrusts represented by the tectonic wedge beneath the front of the Andes between the densely populated cities of San Juan and Mendoza in Argentina is high because these thrust ramps, if continuous, can rupture an area as large as ~7000 km^2 producing an earthquake with a maximum M_w of 7.7. The Pie de Palo blind back thrust area is ~6000 km^2, although the steep segment of the ramp below the eastern flank of the sierra amounts for about 2000 km^2. Fault area of the $M = 7.4$ Caucete event was probably not much larger than 2000 km^2. The low rate of thrust slip documented from geological observations implies long intervals of earthquake recurrence for the basement thrusts documented in this study.

[72] **Acknowledgments.** This is a contribution of Group of Dynamics of the Lithosphere (GDL). We thank Repsol-YPF S.A. for providing us with the seismic lines and for the permission to publish parts of them. This work has been partially supported by 99AR0010 CSIC-CONICET project and Grups de Recerca Consolidats (II Pla de Recerca de Catalunya) Projects 1997 SGR 00020. A.J.M. was supported by U.S. NSF grants EAR-0232603 and EAR-0409443 and a Research Equipment Reserve Fund grant from Oregon State University. The 2DMove software from Midland Valley has been used to identify the best fit for the crustal ramp. We are indebted to Tibor Dunai for analyzing the samples for cosmogenics nuclides from the Cerro Salinas terraces with poor dating results. We also thank Rick Allmendinger for providing the nice satellite images that have been partially reproduced in Figures 3 and 7. We finally thank reviewers Jérome van der Woerd, Gérard Hérail, and Jean-Philippe Avouac for their interesting comments that helped to improve the paper.

References

Allmendinger, R. W., and T. R. Zapata (1996), Imaging the Andean structure of the Eastern Cordillera on reprocessed YPF seismic reflection data paper presented at XIII Congreso Geológico Argentino y III Congreso de Exploración de Hidrocarburos, Univ. de Buenos Aires, Buenos Aires.

Allmendinger, R. W., and T. R. Zapata (2000), The footwall ramp of the Subandean decollement, northernmost Argentina, from extended correlation of seismic reflection data, *Tectonophysics*, *321*, 37–55.

Alonso, J. L., L. R. Rodríquez-Fernández, J. García-Sansegundo, N. Heredia, P. Farias, and J. Gallastegui (2005), Gondwanic and Andean structure in the Argentine central Precordillera: The Río San Juan section revisited paper presented at 6th International Symposium on Andean Geodynamics (ISAG 2005, Barcelona), Universitat Barcelona, Barcelona, Spain.

Alvarado, P., and S. Beck (2006), Source characterization of the San Juan (Argentina) crustal earthquakes of 15 January 1944(M_w 7.0) and 11 June 1952 (M_w 6.8), *Earth Planet. Sci. Lett.*, *243*, 409–423.

Astini, R. A., J. L. Benedetto, and N. E. Vaccari (1995), The early Paleozoic evolution of the Argentine Precordillera as a Laurentian rifted, drifted, and collided terrane: A geodynamic model, *Geol. Soc. Am. Bull.*, *107*, 253–273.

Avouac, J.-P., P. Tapponnier, M. Bai, H. You, and G. Wang (1993), Active thrusting and folding along the northern Tien Shan and late Cenozoic rotation of the Tarim relative to Dzungaria and Kazakhstan, *J. Geophys. Res.*, *98*, 6755–6804.

Bettini, F. H. (1980), Nuevos conceptos tectónicos del centro y borde occidental de la cuenca Cuyana, *Asoc. Geol. Argent. Rev.*, *XXXV*, 579–581.

Brooks, B. A., M. Bevis, R. Smalley Jr., E. Kendrick, R. Manceda, E. Lauría, R. Maturana, and M. Araujo (2003), Crustal motion in the Southern Andes (26°–36°S): Do the Andes behave like a microplate?, *Geochem. Geophys. Geosyst.*, *4*(10), 1085, doi:10.1029/2003GC000505.

Burbank, D., A. Meigs, and N. Brozovic (1996), Interactions of growing folds and coeval depositional systems, *Basin Res.*, *8*, 199–224.

Burbank, D. W., and R. S. Anderson (2001), *Tectonic Geomorphology*, 274 pp., Blackwell Sci., Malden, Mass.

Castellanos, A. (1944), Anotaciones preliminares con motivo de una visita a la ciudad de San Juan a propósito del terremoto del 15 de enero de 1944, Publ. 21, Inst. de Fis. y Geol., Univ. del Litoral, Rosario, Argentina.

Colombo, F., P. Busquets, E. Ramos-Guerrero, J. Vergés, and D. Ragona (2000), Quaternary alluvial terraces in an active tectonic region: The San Juan River Valley, Andean Ranges, San Juan Province, Argentina, *J. South Am. Earth Sci.*, *13*, 611–626.

Cominguez, A. H., and V. A. Ramos (1991), La Estructura Profunda entre Precordillera y Sierras Pampeanas de la Argentina: Evidencias de la Sísmica de Reflexión Profunda, *Rev. Geol. Chile*, *18*, 3–14.

Cortés, J. M., and C. H. Costa (1996), Tectónica cuaternaria en la desembocadura del río de las Peñas, borde oriental de la Precordillera de Mendoza paper presented at XIII Congreso Geológico Argentino y III Congreso de Exploración de Hidrocarburos.

Costa, C. H., and C. Vita-Finzi (1996), Late Holocene faulting in the southeast Sierras Pampeanas of Argentina, *Geology*, *24*, 1127–1130.

Costa, C., T. K. Rockwell, J. D. Paredes, and C. E. Gardini (1999), Quaternary deformations and seismic hazard at the Andean orogenic front (31°–33°, Argentina): A paleoseismological perspective paper presented at Fourth ISAG, Universitaet Goettingen, Goettingen, Germany.

Costa, C. H., C. E. Gardini, H. Diederix, and J. M. Cortés (2000), The Andean orogenic front at Sierra de las Peñas-Las Higueras, Mendoza, Argentina, *J. S. Am. Earth Sci.*, *13*, 287–292.

Cristallini, E. O., and V. A. Ramos (2000), Thick-skinned and thin-skinned thrusting in the La Ramada fold and thrust belt: Crustal evolution of the High Andes of San Juan, Argentina (32°SL), *Tectonophysics*, *317*, 205–235.

Cristallini, E. O., A. H. Comýínguez, V. A. Ramos, and E. D. Mercerat (2004), Basement double-wedge thrusting in the northern Sierras Pampeanas of Argentina (27°S)-Constraints from deep seismic reflection, in *Thrust Tectonics and Hydrocarbon Systems*, edited by K. R. McClay, *AAPG Mem.*, *82*, 65–90.

DeMets, C., R. G. Gordon, D. F. Argus, and S. Stein (1990), Current plate motions, *Geophys. J. Int.*, *101*, 425–478.

Figueroa, D. E., and O. R. Ferraris (1989), Estructura del Margen Oriental de la Precordillera Mendocina-Sanjuanina, Primer Congreso Nacional de Exploración de Hidrocarburos Mar del Plata, Univ. de Buenos Aires, Buenos Aires.

Ford, M., E. A. Williams, A. Artoni, J. Vergés, and S. Hardy (1997), Progressive evolution of a fault-related fold pair from growth strata geometries, Sant Llorenç de Morunys, SE Pyrenees, *J. Struct. Geol.*, *19*, 413–441.

Furque, G., and A. Cuerda (1979), Precordillera de La Rioja, San Juan y Mendoza: Córdoba, Academia Nacional de Ciencias Córdoba paper presented at 2nd Simposio de Geología Regional Argentina, Acad. Nac. de Cien. Córdoba, Córdoba, Argentina.

Galindo, C., C. Casquet, C. Rapela, R. J. Pankhurst, E. Baldo, and J. Saavedra (2004), Sr, C and O isotope geochemistry and stratigraphy of Precambrian and lower Paleozoic carbonate sequences from the Western Sierras Pampeanas of Argentina: Tectonic implications, *Precambrian Res.*, *131*, 55–71.

Gimenez, M. E., M. P. Martínez, and A. Introcaso (2000), A crustal model based mainly on gravity data in the area between the Bermejo Basin and the Sierras de Valle Fértil, Argentina, *J. South Am. Earth Sci.*, *13*, 275–286.

González Bonorino, G. (1973), Sedimentología de la Formación Punta Negra y algunas consideraciones sobre la geología regional de la Precordillera de San Juan y Mendoza, *Asoc. Geol. Argent. Rev.*, *30*, 223–246.

Groeber, P. (1944), Movimientos tectónicos contemporáneos y un nuevo tipo de dislocaciones, *Not. Museo La Plata*, *9*, 363–375.

Hubert-Ferrari, A., J. Suppe, X. Wang, and C. Z. Jia (2005), Yakeng detachment fold, South Tianshan, China, in *Seismic Interpretation of Contractional Fault-related Folds, AAPG Seismic Atlas*, edited by J. Shaw, C. Connors, and J. Suppe, pp. 110–113, Am. Assoc. of Pet. Geol., Tulsa, Okla.

Hubert-Ferrari, A., J. Suppe, R. Gonzalez-Mieres, and X. Wang (2007), Mechanisms of active folding of the landscape (southern Tian Shan, China), *J. Geophys. Res.*, doi:10.1029/2006JB004362, in press.

Instituto Nacional de Prevención Sísmica (INPRES) (1982), Microzonación Sísmica del Valle de Tulum - Provincia de San Juan, Informe Técnico General, vol. 1–3.

Instituto Nacional de Prevención Sísmica (INPRES) (1995), Microzonificación Sísmica del Gran Mendoza. Resumen Ejecutivo, publicación técnica, 283 pp., San Juan, Argentina.

Introcaso, A., M. C. Pacino, and H. Fraga (1992), Gravity, isostasy and Andean crustal shortening between latitudes 30° and 35°S, *Tectonophysics*, *205*, 31–48.

Irigoyen, M. V., M. E. Villeneuve, and F. Quigg (1999), Calibration of a Neogene magnestostratigraphy by ^{40}Ar-^{39}Ar geochronology: The foreland basin strata of northern Mendoza Province, Argentina, in *Radiogenic Age Isotopic Studies, Current Research 1999-F*, *Rep. 12*, pp. 27–41, Geol. Surv. of Can., Ottawa, Ont.

Irigoyen, M. V., K. L. Buchan, and R. L. Brown (2000), Magnetostratigraphy of Neogene Andean foreland-basin strata, latitude 33°S, Mendoza Province, Argentina, *Geol. Soc. Am. Bull.*, *112*, 803–816.

Isacks, B., T. Jordan, R. W. Allmendinger, and V. A. Ramos (1982), La segmentación tectónica de los Andes Centrales y su relación con la placa de Nazca subductada, Vth Congreso Latinoamericano de Geología, Univ. de Buenos Aires, Buenos Aires.

Jordan, T. E., and R. W. Allmendinger (1986), The Sierras Pampeanas of Argentina: A modern analogue of Rocky Mountain foreland deformation, *Am. J. Sci.*, *286*, 737–764.

Jordan, T. E., B. Isacks, R. W. Allmendinger, I. A. Brewer, V. Ramos, and C. J. Ando (1983), Andean tectonics related to geometry of subducted Nazca Plate, *Geol. Soc. Am. Bull.*, *94*, 341–361.

Kadinsky-Cade, K., R. Reilinger, and B. Isacks (1985), Surface deformations associated with the November 23, 1977, Caucete, Argentina, earthquake sequence, *J. Geophys. Res.*, *90*, 12,691–12,700.

Kay, S. M., and J. M. Abbruzzi (1996), Magmatic evidence for Neogene lithospheric evolution of the central Andean "flat-slab" between 30°S and 32°S, *Tectonophysics*, *259*, 15–28.

Kendrick, E. C., M. Bevis, R. F. Smalley Jr., O. Cifuentes, and F. Galban (1999), Current rates of convergence across the central Andes: Estimates from continuous GPS observations, *Geophys. Res. Lett.*, *26*, 541–544.

Krugh, W. C. (2003), Fold growth due to kink-band migration in repeated earthquakes, Sierra de Villicum, San Juan, Argentina., Master's thesis, 54 pp., Oregon State Univ., Corvallis.

Marrett, R., and P. A. Bentham (1997), Geometric analysis of hybrid fault-propagation/detachment folds, *J. Struct. Geol.*, *19*, 243–248.

Martos, L. M. (1993), Evidencias de actividad tectónica en el Pleistoceno superior-Holoceno, Quebrada del Molino, Pocito, San Juan, Argentina paper presented at Congreso Geológico Argentino, Congr. Geol. Argent., Buenos Aires.

Martos, L. M. (1995), Análisis morfo-estructural de la faja piedemontana oriental de las sierras deMarquesado, Chica de Zonda y Pedernal: Su aplicación para prevenir riesgos geológicos: Provincia de San Juan, Ph.D. thesis, 554 pp., Univ. Nac. de San Juan, San Juan, Argentina.

Meigs, A., W. C. Krugh, C. Schiffman, J. Vergés, and V. Ramos (2007), Refolding of thin-skinned thrust sheets by active basement-involved thrust faults in the eastern Precordillera of western Argentina, in *Andean Neotectonics*, edited by C. Costa, *Rev. Asoc. Geol. Argent.*, in press.

Meyer, B., P. Tapponnier, L. Bourjot, F. Métivier, Y. Gaudemer, G. Peltzer, G. Shummin, and C. Zhitai (1998), Crustal thickening in Gansu-Qinghai, lithospheric mantle subduction, and oblique, strike-slip controlled growth of the Tibet Plateau, *Geophys. J. Int.*, *135*, 1–47.

Molnar, P., E. T. Brown, B. C. Burchfiel, Q. Deng, X. Feng, J. Li, G. M. Raisbeck, J. Shi, Z. Wu, F. Yiou, and H. You (1994), Quaternary climate change and the formation of river terraces across growing anticlines on the north flank of the Tien Shan, China, *J. Geol.*, *102*, 583–602.

Novoa, E., J. Suppe, and J. H. Shaw (2000), Inclined-shear restoration of growth folds, *AAPG Bull.*, *84*, 787–804.

Pankhurst, R. J., C. W. Rapela, J. Saavedra, E. Baldo, J. Dahlquist, I. Pascua, and C. M. Fanning (1998), The Famatinian magmatic arc in the central Sierras Pampeanas, in *The Proto-Andean Margin of Gondwana*, edited by R. J. Pankhurst and C. W. Rapela, *Geol. Soc. Spec. Publ.*, *142*, 343–368.

Piñán-Llamas, A., and C. Simpson (2006), Deformation of Gondwana margin turbidites during the Pampean orogeny, north-central Argentina, *Geol. Soc. Am. Bull.*, *118*, 1270–1270, doi:10.1130/B25915.1.

Pratt, T. L., J. H. Shaw, J. F. Dolan, S. A. Christofferson, R. A. Williams, J. K. Odum, and A. Plesch (2002), Shallow seismic imaging of folds above the Puente Hills blind-thrust fault, Los Angeles, California, *Geophys. Res. Lett.*, *29*(9), 1304, doi:10.1029/2001GL014313.

Ragona, D., G. Anselmi, P. González, and G. Vujovich (1995), Mapa geológico de la Provincia de San Juan, República Argentina, scale 1/500,000, Secret. de Miner., Dir. Nac. del Serv. Geol., Buenos Aires.

Ramos, V. A. (1988), The Tectonics of the Central Andes; 30° to 33° S latitude, in *Processes in Continental Lithospheric Deformation*, edited by S. P. Clark, J. B. Clark Burchfiel, and J. Suppe, pp. 31–54, Geol. Soc. of Am., Boulder, Colo.

Ramos, V. A., and G. Vujovich (2000), Hoja Geológica San Juan, *Serv. Geol. Min. Argent. Bol.*, *245*, 1–82.

Ramos, V. A., T. E. Jordan, R. W. Allmendinger, C. Mpodozis, S. M. Kay, J. M. Cortés, and M. A. Palma (1986), Paleozoic terranes of the central Argentine-Chilean Andes, *Tectonics*, *5*, 855–880.

Ramos, V. A., M. Cegarra, G. Lo Forte, and A. Comínguez (1997), El frente orogénico en las Sierras de Pedernal (San Juan, Argentina): Su migración a través de los depósitos sinorogénicos paper presented at Simposio Final Proyecto IGCP 345 Evolución Litosférica de los Andes, Antofagasta, Chile.

Ramos, V. A., R. D. Dallmeyer, and G. I. Vujovich (1998), Time constraints on the early Paleozoic docking of the Precordillera, central Argentina, in *The Proto-Andean Margin of Gondwana*, edited by R. J. Pankhurst and C. W. Rapela, *Geol. Soc. Spec. Publ.*, *142*, 143–158.

Ramos, V. A., E. O. Cristallini, and D. J. Pérez (2002), The Pampean flat-slab of the central Andes, *J. South Am. Earth Sci.*, *15*, 59–78.

Ramos, V. A., T. Zapata, E. Cristallini, and A. Introcaso (2004), The Andean thrust system—Latitudinal variations in structural styles and orogenic shortening, in *Thrust Tectonics and Hydrocarbon Systems*, edited by K. R. McClay, *AAPG Mem.*, *82*, 30–50.

Regnier, M., J.-L. Chatelain, R. F. Smalley Jr., J. Ming Chiu, and B. L. Isacks (1992), Seismotectonic of the Sierra Pie de Palo, a basement block uplift in the Andean foreland, Argentina, *Bull. Seismol. Soc. Am.*, *82*, 2549–2571.

Shaw, J., C. Connors, and J. Suppe (2005), *Seismic Interpretation of Contractional fault-Related Folds*, *AAPG Seismic Atlas, Stud. Geol.*, vol. 53, pp. 1–156, Am. Assoc. of Pet. Geol., Tulsa, Okla.

Shaw, J. H., and J. Suppe (1996), Earthquake hazards of active blind-thrust under the central Los Angeles basin, California, *J. Geophys. Res.*, *101*, 8623–8642.

Siame, L., O. Bellier, M. Sébrier, D. Bourlès, P. Leturmy, M. Perez, and M. Araujo (2002), Seismic hazard reappraisal from combined structural geology, geomorphology and cosmic ray exposure dating analyses: The Eastern Precordillera thrust system (NW Argentina), *Geophys. J. Int.*, *150*, 241–260, doi:210.1046/j.1385-1246X. 2002.01701.x.

Siame, L. L., O. Bellier, M. Sébrier, and M. Araujo (2005), Deformation partitioning in flat subduction setting: Case of the Andean foreland of western Argentina (28°S–33°S), *Tectonics*, *24*, TC5003, doi:10.1029/2005TC001787.

Smalley, R. F., Jr., and B. L. Isacks (1987), A high resolution local network study of the Nazca Plate Wadati-Benioff zone under western Argentina, *J. Geophys. Res.*, *92*, 13,903–913,913.

Smalley, R. F., Jr., and B. L. Isacks (1990), Seismotectonics of thin- and thick-skinned deformation in the Andean Foreland from local network data: Evidence for a seismogenic lower crust, *J. Geophys. Res.*, *95*, 12,487–12,498.

Smalley, R. J., J. Pujol, M. Regnier, J.-M. Chiu, J.-L. Chatelain, B. L. Isacks, M. Araujo, and N. Puebla (1993), Basement seismicity beneath the Andean Precordillera thin-skinned thrust belt and implications for crustal and lithospheric behavior, *Tectonics*, *12*, 63–76.

Snyder, D. B., V. A. Ramos, and R. W. Allmendinger (1990), Thick-skinned deformation observed on deep seismic reflection profiles in western Argentina, *Tectonics*, *9*, 773–788.

Suppe, J. (1983), Geometry and kinematics of fault-bend folding, *Am. J. Sci.*, *283*, 684–721.

Suppe, J., G. T. Chou, and S. C. Hook (1992), Rates of folding and faulting determined from growth strata, in *Thrust Tectonics*, edited by K. R. McClay, pp. 105–121, CRC Press, Boca Raton, Fla.

Suppe, J., F. Sàbat, J. A. Muñoz, J. Poblet, E. Roca, and J. Vergés (1997), Bed-by-bed fold growth by kink-band migration: Sant Llorenç de Morunys, eastern Pyrenees, *J. Struct. Geol.*, *19*, 443–461.

Tassara, A. (2005), Interaction between the Nazca and South American plates and formation of the Altiplano–Puna plateau: Review of a flexural analysis along the Andean margin (15°–34°S), *Tectonophysics*, *399*, 39–57.

Uliarte, E., H. Bastías, and L. Ruzycki (1987), Morfología y neotectónica en el Cerro La Chilca, Pedernal, Provincia de San Juan, Argentina paper presented at X Congreso Geológico Argentino, Univ. Nac. de Tucumán, San Miguel de Tucuman, Argentina.

Vergés, J., E. Ramos-Guerrero, D. Seward, P. Busquets, and F. Colombo (2001), Miocene sedimentary and tectonic evolution of the Andean Precordillera at 31°S, Argentina, *J. S. Am. Earth Sci.*, *14*(7), 735–750.

Vergés, J., V. Ramos, F. H. Bettini, A. Meigs, E. Cristallini, A. L. Cortés, and T. Dunai (2002), Geometría y edad del anticlinal fallado de Cerro Salinas, in *Actas del XV Congreso Geológico Argentino, El Calafate* [CD-ROM], edited by N. Cabaleri et al., paper 358, Congr. Geol. Argent., El Calafate, Argentina.

von Gosen, W. (1992), Structural evolution of the Argentine Precordillera: The Rio San Juan section, *J. Struct. Geol.*, *14*, 643–667.

Vujovich, G., and V. Ramos (1994), La faja de Angaco y su relación con las Sierras Pampeanas Occidentales paper presented at 7th Congreso Geológico Chileno, Univ. de Concepción, Concepción, Chile.

Wells, D. L., and K. J. Coppersmith (1994), New empirical relationships among magnitude, rupture length, rupture width, rupture area, and surface displacement, *Bull. Seismol. Soc. Am.*, *84*, 974–1002.

Yeats, R. S. (1986), Active faults related to folding, in *Active Tectonics*, edited by R. E. Wallace, pp. 63–79, Natl. Acad. Press, Washington, D. C.

Yeats, R. S., and G. J. Huftile (1995), The Oak Ridge faults system and the 1994 Northridge earthquake, *Nature*, *373*, 418–420.

Yrigoyen, M. R. (1993), Los depósitos sinorogénicos terciarios, in Geología y recursos naturales de la provincia de Mendoza, in *XII Congreso Geológico Argentino y II Congreso de Exploración de Hidrocarburos*, edited by V. A. Ramos, pp. 123–148, Congr. Geol. Argent., Buenos Aires.

Zapata, T. (1997), Geometria y Evolución de la Estructura Cortical de la Precordillera Oriental y Valle del Bermejo a los 30° de Latitud Sur, *Bol. Inf. Petrol.*, *49*, 84–104.

Zapata, T. R. (1998), Crustal structure of the Andean thrust front at 30(S latitude from shallow and deep seismic reflection profiles, Argentina, *J. S. Am. Earth Sci.*, *11*, 131–151.

Zapata, T. R., and R. W. Allmendinger (1996a), Growth stratal records of instantaneous and progressive limb rotation in the Precordillera thrust belt and Bermejo basin, Argentina, *Tectonics*, *15*, 1065–1083.

Zapata, T. R., and R. W. Allmendinger (1996b), Thrust-front zone of the Precordillera, Argentina: A thick-skinned triangle zone, *AAPG Bull.*, *80*, 359–381.

F. H. Bettini, Repsol-YPF, Av. Pte. Roque Sáenz Peña 777, 1035 Buenos Aires, Argentina. (fbettinim@repsolypf.com)

J. M. Cortés, E. Cristallini, and V. A. Ramos, Laboratorio de Tectónica Andina, Departamento de Ciencias Geológicas, Universidad de Buenos Aires, 1428 Buenos Aires, Argentina. (andes@gl.fcen.uba.ar)

A. Meigs, Department of Geosciences, Oregon State University, Corvallis, OR 97331, USA. (meigsa@geo.oregonstate.edu)

J. Vergés, Group of Dynamics of the Lithosphere (GDL), Institute of Earth Sciences "Jaume Almera", CSIC, E-08028 Barcelona, Spain. (jverges@ija.csic.es)